THE EFFECTS OF NOISE IN CATV DISTRIBUTION NETWORKS WITH STAR COUPLERS AND FIBER AMPLIFIERS

by

David Yong Chen

Thesis submitted to the Faculty of

Virginia Polytechnic Institute and State University

in partial fulfillment of the requirements for the degree of

Master of Science

in

Electrical Engineering

APPROVED BY:

Ira Jacobs

Dr. Ira Jacobs, Chairman

A. Safaai-Jazi

Dr. Ahmad Safaai-Jazi

Brian D. Woerner

Dr. Brian D. Woerner

September, 1994

Blacksburg, Virginia

THE EFFECTS OF NOISE IN CATV DISTRIBUTION NETWORKS WITH STAR COUPLERS AND FIBER AMPLIFIERS

by
David Y. Chen
Dr. Ira Jacobs, Chairman

ABSTRACT

Noise and distortion limit the channel capacity and degrade the system performance in AM-VSB SCM CATV Distribution Networks. The use of star couplers and fiber amplifiers is an approach to overcome these problems and meet the increasing demand for large capacity and high quality.

The capacity and performance analysess of three different network configurations are compared based on the results of computer modeling. In practice, the best configuration depends on the optical amplifiers and the pump lasers used in the system as well as the requirement on the number of channels and the number of subscribers. It is found that in a two-stage star network the largest improvement in the capacity and performance may be achieved when the optical amplifiers between the stages are individually pumped. For example, a capacity of 200 channels and 572 output nodes may be obtained. There is an optimal length of the erbium-doped fiber amplifier (EDFA) and there is also an optimal position where the EDFA is located between the two star couplers.

The modeling is based on an extensive analysis of noise and distortion in the system. A discrepancy in the power behavior of laser relative intensity noise (RIN) is pointed out. A previous analysis on reflection induced noise is extended to include the effect of quadruply-reflected light and optical amplifiers. Since chirp-dispersion distortion and gain tilt distortion are found to be negligible, clipping distortion is the main limitation on the system capacity. Optical amplifier noise provides an additional limitation to the system. Because the gain and amplified spontaneous noise depend on the input signal power and pump power, the gain and spontaneous emission factor are modeled for the comparison of the different systems.

ACKNOWLEDGEMENTS

I would like to express my greatest thanks to my advisor Dr. Ira Jacobs for his excellent guidance and constant support throughout my work. I feel lucky and proud to be his student. It has been a very rewarding experience working with him as his student.

I wish to thank Dr. Safaai-Jazi and Dr. Woerner for being my graduate committee members and offering their helpful insight. I also wish to thank the other professors who have given me great instruction at Virginia Tech. I am grateful to Mr. Joe Wiencko for his kind assistance and guidance. I would also like to thank all my friends at Virginia Tech for the good times they provided

My special thanks go to my best friend, David Quan Chen, who is living in another world. Our eternal friendship is always a strong encouragement to me.

Finally, I am extremely grateful to my parents, sister and brother, who have sacrificed so much to support my study in the United States.

THE EFFECTS OF NOISE IN CATV DISTRIBUTION NETWORKS WITH STAR COUPLERS AND FIBER AMPLIFIERS

TABLE OF CONTENTS

LIST OF FIGURES

LIST OF TABLES

INTRODUCTION

CHAPTER 1 INTRODUCTION

With the great development of lightwave technologies, fiber optic transmission becomes a necessary and feasible approach to meet the demand for fast, high-quality and huge-volume communications in the age of information. The eventual goal of transmission technology is to make the communication media transparent, like the crystal glass, and almost costless. This dream can only be realized by the tiny hair-like crystal thread, the optical fiber. Optical fibers will take the place of coaxial cables or copper wires to be the core of the communication systems of the whole world in the near future.

Cable television (CATV) distribution networks are one of the most important applications of optical fibers. Because of the high demand for interactive video distribution and integrated services, lightwave CATV networks have been widely researched and are likely to be commercially deployed in the near future. This broadband network may revolutionize the CATV and telecommunications industries. In order to have a good-quality and cost-effective system, we need to understand the characteristics of noise and distortion in such systems to make an optimum design. This is the motivation and task of this thesis.

Building on results published in the literature, we present a new configuration for CATV distribution networks--*amplitude-modulation vestigial sideband subcarrier multiplexed* (AM-VSB SCM) two-stage star CATV distribution network with fiber amplifiers. By analyzing and modeling the impairment of noise and distortion, we estimate the capacity and performance of different configurations for the lightwave CATV distribution network. Also, we find the optimum configuration for specific circumstances from the modeling results. We hope our work could be a reference for the implementation of practical CATV distribution systems.

1.1 Current Status of Multichannel CATV Distribution Systems

Most of the current multichannel CATV distribution is presently done by coaxial cables. The television signals are transmitted in the North American *National Television Systems Committee Amplitude Modulated Vestigial Sideband* (NTSC AM-VSB) TV format. The advantages of the AM-VSB technique are the low-bandwidth requirement and simplicity of the electronic circuits. A number of CATV channels are located at a number of assigned frequency slots, which is known as *frequency division multiplexing (FDM).* All of the channels are transmitted to each subscriber, who access the wanted channel through a CATV converter box. Although the coaxial systems are very cost-effective, there are a few critical limitations which may make them obsolete for future broadband services.

First, the bandwidth which can be used for good quality transmission is very limited in coaxial cables. Second, the signal loss in the cables is quite high. The electronic repeater amplifiers are employed to compensate the signal loss of coaxial cables and splitting losses. But they add noise and nonlinear distortion, thus degrading the signal quality. Also, the amplifiers contain active components and must be provided with electrical power. This reduces the system reliability and may cause a lot of installation problems and high maintenance expenses. The maximum number of channels which may be transmitted to the receiver with good quality is only about 50. This limit has been reached by the commercial CATV systems. With the increasing demand for more channels (500 channels expected), it is inevitable to make a change in the transmission media.

Therefore, a fiber optic system with high capacity, low signal loss and high reliability is the desired approach for new CATV distribution systems.

1.2 Review of Lightwave Multichannel CATV Distribution System

For lightwave multichannel CATV distribution systems, AM-VSB with subcarrier multiplexing (SCM) technique is an attractive solution for broadcasting hundreds of channels to a large number of subscribers, owing to their convenient interface with standard CATV multiplexing and coaxial cable transmission. In SCM systems, different channels are produced by modulating different radio frequency (RF) carriers and are combined to modulate a single optical carrier. Different microwave carriers are demultiplexed at the receiver using standard RF techniques. The SCM technique provides the system with flexibility and upgradability. Either analog or digital modulation, or a combination of the two, can be used to transmit multiple voice, data and video signals to a large number of subscribers. The basic architecture of a SCM lightwave system is described in Section 2.1.

In 1986-87, several experiments on high performance SCM systems were reported. Darcie et al. of AT&T Bell Laboratories demonstrated subcarrier multiplexing for an optical multiple-access-network [1]. Olshansky and Lanzisera of GTE Laboratories reported a 60-channel FM video SCM transmission system [2]. Way et al. of *Bell Communications Research* (Bellcore) used the SCM technique in a microwave multicarrier transmission link [3]. Since then, significant improvement in the opto-electronic devices for these systems have been made, bringing the systems closer to the commercial stage. For example, the commercialization of the *distributed-feedback* (DFB) laser provides high linearity, high optical power and extremely low *relative intensity noise* (RIN), overcoming the three big problems in analog lightwave systems. In one AM-VSB experiment, 42 video channels with 6MHz channel spacing were transmitted by using subcarriers in the 50-400MHz frequency range [4]. These systems were operated at near-shot-noise-limit.

1.3 Limitations in Lightwave AM-VSB SCM CATV System

As first demonstrated by A. Saleh of AT&T Bell Laboratories [5], the threshold nonlinearity of laser diodes is a fundamental limit on the channel capacity of AM SCM systems. The threshold nonlinearity is the result of the modulating current being less than the laser threshold current at some times when the number of channels is large. In such cases, the input signals get clipped and this results in clipping distortion. This will be described more in Section 3.2.1. In order to calculate the channel capacity, Saleh considered the nonlinear distortion as a noise power which degrades the system performance. However, the performance requirement in CATV systems are given separately for noise and nonlinear distortion. So his consideration may be inappropriate and lead to an under-estimation of the channel capacity, as implied by the experiment reported by M. Tanabe et al. [6]. C. J. Chung and I. Jacobs [7] demonstrated from both experiment and simulation that the nonlinear distortion should be considered differently from the noise. They showed that the laser RMS modulation index μ should not exceed about 0.3 in order that the nonlinear distortion due to the threshold nonlinearity of laser diodes not exceed the CATV requirements. The RMS modulation index is given by $\mu = m\sqrt{N/2}$, where m is the modulation index per channel and N is the number of channels.

A high *carrier-to-noise ratio* (CNR) is required for the AM SCM signal transmission. Since the total modulation index is limited and the modulation index per channel needs to be above a certain value to provide large enough CNR, the number of channels is limited at less than 100 channels. Also, the limit on the modulation index sets a strict power budget and limits the number of subscribers accommodated. In order to transmit hundreds of channels to a large number of subscribers, we consider employing star couplers, as *wavelength division multiplexing* (WDM) devices and power splitters, and erbium doped fiber amplifiers (EDFAs), as power boosters to compensate the distribution losses.

1.4 Improvement by the Use of Fiber Amplifiers and Star Couplers

Since the late 1980s, the advent of *erbium-doped fiber amplifiers* (EDFAs) has created a big impetus for lightwave systems. An experiment in which 19 AM-VSB video channels were transmitted by using an erbium-doped fiber amplifier was reported by a group at Bellcore [8]. In 1991, Gabla, et al.[9] used the fiber amplifier to boost the output power to 11dBm so that the power budget of 35-channel AM-VSB, SCM system was 16dB. The EDFAs, with high gain, low noise and their immunity to interchannel crosstalk, allow large distribution losses to be compensated and aid the development of lightwave multichannel CATV systems.

Even after the EDFAs are used to improve the performance and capacity of the system, the channel capacity is still limited by the nonlinearity of laser diodes. To provide a large number of channels to subscribers at the same time, we may use the WDM technique, where several different optical wavelengths are combined in the same system. However, the fiber amplifiers add *amplified spontaneous emission* (ASE) noise as well as gain-tilt distortion, and they set a new limit on the capacity in term of either the number of channels or the number of subscribers.

1.5 Organization of This Thesis

We have briefly introduced the motivation of the thesis and the current status of the CATV distribution systems in this introduction. The remainder of this thesis is divided into two parts: applications and theories.

Part A, the application level, proposes the network configurations and analyzes their capacities and performances. It contains three chapters. In chapter 2, three different network configurations are described. Their advantages and disadvantages are pointed out and compared. The following two chapters, Chapter 3 and 4, further compares these configurations by numerical modeling. The relation of the number of channels and the number of subscribers, the relation of the noise performance and the capacity, and the effect of the optical amplifier pump power on the system are determined by numerical evaluation. Optimum configurations are identified.

The basis of the results of Part A, the theories of noise and distortion, and computer modeling, is described in Part B. The physics of laser intrinsic RIN is first investigated. We point out a discrepancy in the literature about the behavior of RIN at low frequency. After that, the characteristics of another relative intensity noise, reflection induced noise, is summarized and analyzed with a higher order approximation than appears in the literature. Later in Chapter 5, amplified spontaneous emission noise, which is of most concern in this thesis, is described. At the end of Chapter 5, the enhancement of noise due to the amplifier is shown analytically. Chapter 6 deals with three kinds of nonlinear distortion in the system. First, clipping distortion, which is the fundamental limit in AM SCM multichannel systems, is studied conceptually. The basic concept of chirp-dispersion distortion is introduced, and nonlinear distortion due to the coupling of gain-tilt and chirp is investigated. Finally, we describe the modeling of the gain and the spontaneous emission factor of the fiber amplifiers, the results of which are used in the computation of the performance of distribution networks in Part A.

PART A TWO-STAGE STAR CATV DISTRIBUTION NETWORK WITH EDFAs

CHAPTER 2 NETWORK CONFIGURATIONS

In this chapter, three configurations of networks with fiber amplifiers are described. The baseline configuration consists of a source laser diode, followed by an EDFA with a pump laser and a 1XK star coupler. Adding an MXM star, more source lasers and EDFAs as needed, a two-star single-pump configuration is formed. This configuration uses wavelength division multiplexing and only one pump laser is required. The third configuration is the same as the second except that the EDFAs are pumped separately (multipump case). This configuration, as will be shown, provides a significant improvement over the first two configurations. These three configurations are described more fully, and their performance evaluated, in the following chapters.

2.1 Baseline:

A basic CATV distribution network is shown in Figure 2.1. N subcarriers are each modulated by an input AM-VSB CATV signal, and the outputs of all modulated subcarriers are summed by using an RF power combiner. The combined signal is used to intensity modulate the source laser diode. The output light is amplified by an EDFA and transmitted to the receiver through the single-mode fiber. A 1XK splitter is used to split the signal and distribute it to every output optical node. Only one wavelength is used and therefore only one photodetector is required at each optical node. A PIN photodetector instead of an APD is chosen because shot noise is larger than thermal noise in the system. The photodetector gives an electrical current output proportional to the optical power input. The proportionality constant is the responsivity of the detector, which for good PINs at 1.3μm is about R=0.93mW/mA. The output electrical signal is the combination of all N channels with different subcarrier frequencies. The CATV signal of each channel is obtained by demodulation and is available to each subscriber through an appropriate video switch. Note that the switch may be either at a remote location or in a TV set-top converter as in typical CATV applications.

2.2 Single-pump:

Figure 2.2 is the structure of a CATV distribution network employing two-stage star couplers and EDFAs with a single pump laser. The network is formed by using one input-stage MXM coupler, M output-stage 1XK couplers (splitters), and M EDFAs connecting the input-stage coupler to each output-stage coupler. The first-stage star functions both as a WDM combiner (each laser is at a different wavelength) and power splitter while the second-stage stars function as splitters. Each input signal appears at all MK output ports with its power divided by MK and with each EDFA adding both gain (G) and noise power (σ_A^2/K). The M EDFAs are pumped by a pump laser connected to one input port of the first-stage coupler. The pump power at each EDFA is the total power reduced by the splitting loss and excess loss of the first star coupler.

The input signal at the input ports of the first star is produced by the SCM technique from a number of AM-VSB signals, as in the baseline case. Consequently, the total number of input channels is (M-1)N (N is the number of channels multiplexed at each input port), and the total number of output nodes is MK. At each output node, the signals at different wavelengths are separated by a WDM demultiplexing device. Each photodiode receives the light with a specific wavelength and converts it to the electrical signal. With further electrical splitting, each output optical node could serve more than one subscriber. Subscribers might access the (M-1)N channels by a video switch located at the output node.

2.3 Multiple-pump:

The two configurations considered above require only one pump laser. However, the power of the pump laser is limited, and the pump power entering each EDFA may be too low after splitting in the case of the single pump configuration. A significant improvement can be achieved by using multiple pump lasers--each EDFA being pumped by one pump laser. Since the EDFA is now pumped by a larger power, a higher gain and smaller spontaneous emission factor may be achieved. The only change from the above configuration is that all M input ports are used for the source lasers and each pump laser is pumped by an EDFA after the first-stage star. It will be shown that the capacity and performance of this configuration are significantly better than both the baseline and single-pump configurations.

In this system, M EDFAs, M pump lasers and M source lasers are needed. Since the pump power at each EDFA is now independent of the number of ports of the first-stage star, there is no strict limit on the number of ports of the star as far as pumping is concerned. Therefore, more channels may be accommodated by increasing the number of input ports. However, if more wavelengths are used, more photodetectors are required at each output node and the video switches will be more complicated. Also, the larger the value of M, the more severe are the requirements on laser wavelength stability and on the resolution of the wavelength demultiplexing filter. We will show that the M=4 network provides a possible capacity of 560 channels, large enough for at least near-future video-on-demand. Therefore, larger M may be unnecessary.

2.4 Review of Other Network Configurations:

Before the invention of the EDFAs, distribution networks were very limited. The configuration of a two-stage star can not be implemented without fiber amplifiers because of the large splitting loss and high CNR requirement. Therefore, the capacity in terms of either the number of channels or the number of subscribers is very limited. The number is less than 100 if a single wavelength is used [5] [7].

A symmetric two-stage star network with EDFAs was first presented by Willner [10], as shown in Figure 2.3. There are K MXM first-stage stars and M KXK second-stage stars with MK EDFAs between them. One of the input ports of each first stage star is used for the pump laser. Consequently, K(M-1) source lasers are required. This is a symmetric structure having the same number of input and output ports, which is advantageous in telephone and computer network applications. The disadvantages of this configuration for CATV application, where more output than input ports are needed, are: first, too many EDFAs and star couplers are required; second, the number of output nodes is relatively small; third, important for the large-gain case, the amplified spontaneous emission noise from different EDFAs adds in the second-stage star.

2.5 Network Parameters

The values of the parameters of both the passive and active devices in the practical system may vary depending on the system. Here we choose typical values to get a representative result. The value of RIN includes the laser relative intensity noise and the reflection induced noise. In equations, RIN denotes the spectral density of this noise. Assuming that optical isolators are used to reduce the reflection induced noise, we choose a small value of RIN. All the power of the active devices are the values after experiencing the insertion loss. The excess loss of the star coupler actually depends on the number of ports of the star coupler and manufacturing process. The absorption coefficient and the intrinsic saturation power are determined by the material, doping density and fiber structure. Table 2.1 lists the typical values of the parameters of the system[11]. These parameters will be used in Chapter 3 and Chapter 4 to evaluate and compare the capacity and performance of the various network configurations.

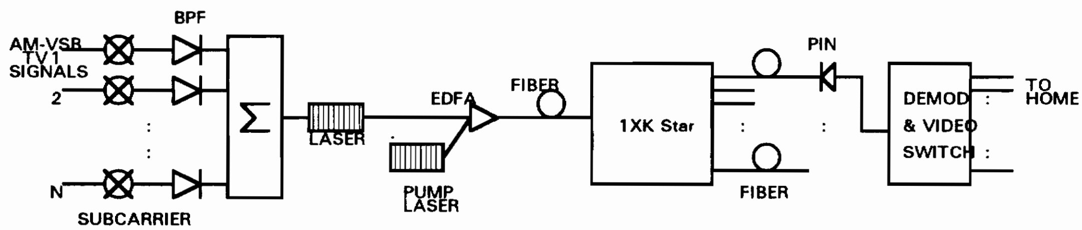

FIGURE 2.1 BASIC LIGHTWAVE CATV DISTRIBUTION NETWORK.

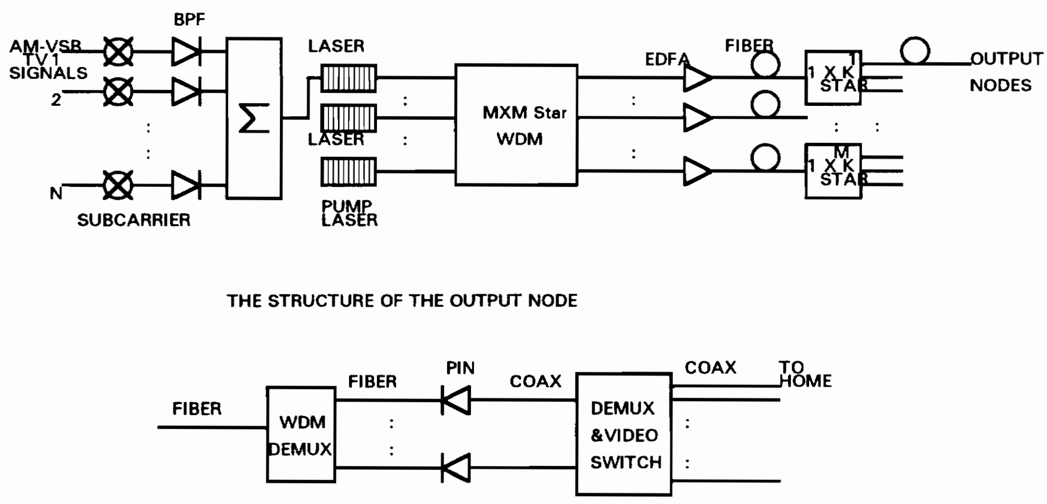

FIGURE. 2.2 STRUCTURE OF CATV DISTRIBUTION NETWORK WITH A SINGLE PUMP LASER
An MXM star coupler, followed by M EDFAs and M 1XK star couplers, functions both as a WDM combiner and as a power splitter. One of the input ports of each first stage star is for a pump laser, the others for laser diodes with different wavelengths. The pump power is distributed to M EDFAs. At each output node, a WDM dumultiplexer separates the light of different wavelengths to different PIN receivers. The electrical demultiplexer and video switch receives the electrical signals and makes N(M-1) channels available to each subscriber.

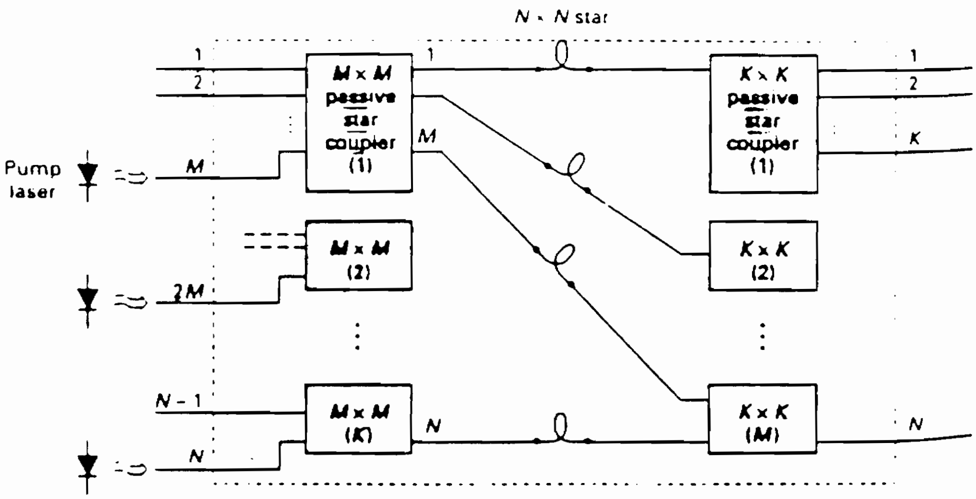

Active $N \times N$ star coupler made from K ($M \times M$) stars, K pump laser diodes, N lengths of doped fiber, and M ($K \times K$) stars. $N = KM$.

FIGURE 2.3 SYSMMETRIC TWO-STAGE STAR NETWORK WITH EDFAs (TAKEN FROM [10])

TABLE 2.1 Typical Parameters of the Network

Parameters	Symbols	Typical values
Excess loss of star coupler	L	~1dB
Relative Intensity Noise	RIN	-155dB/Hz
Spontaneous Emission Factor	n_{sp}	Calculated
Responsivity of the Receiver	R	0.93A/W
Photocurrent of Thermal Noise	$(<i_{th}^2>/B_e)^{1/2}$	$7pA/(Hz)^{1/2}$
Receiver Bandwidth	Be	4MHz
Pump Power	Pp	200mW
Optical Bandwidth	Bo	10GHz(0.07nm)
Fiber Amplifier Gain	G	Calculated
Output Power of Lasers	P	5mW
Intrinsic Saturation Powers	P_{sat}	0.549mW(Pump)/0.272mW(Signal)
Absorption Constant	a_a	0..792m^{-1}(Pump)/0.876m^{-1}(Signal)

CHAPTER 3 SYSTEM CAPACITY ANALYSIS

As mentioned in Chapter 1, the nonlinearity of laser diodes sets a fundamental limit on the capacity of multichannel AM SCM lightwave systems. In the systems we consider here, the amplified spontaneous emission noise contributes additionally to the limit as an impairment. The magnitude of the pump power in the single-pump configuration has a significant effect on the capacity in terms of the number of channels that may be obtained. A large improvement in the capacity may be achieved in the multiple-pump configuration.

3.1 The Expression for the Capacity

The carrier-to-noise ratio at the direct-detection receiver of the two-stage star distribution system given in Figure 2.2 is [12]

$$CNR = \frac{1/2m^2(L_1L_2GRP_s/(MK))^2}{(<i_{th}^2> + <i_{sh}^2> + <i_{rin}^2> + <i_{s-sp}^2> + <i_{sp-sp}^2>)}, \qquad (3.1)$$

where the first term in the denominator is the thermal noise, the second is the shot noise, and the other terms are respectively the relative intensity noise, the signal-spontaneous beat noise and the spontaneous-spontaneous beat noise. They may be represented as [12][13]

$$<i_{s-sp}^2> = 4R^2h\nu n_{sp}(G-1)GL_1L_2^2P_sB_e/(MK^2)$$

$$<i_{sp-sp}^2> = 4[Rh\nu n_{sp}(G-1)L_2/K]^2B_eB_o$$

$$<i_{sh}^2> = 2qRGL_1L_2(P_s+P_{ASE})B_e/(MK)$$

$$<i_{th}^2> = 4kTB_e/R_e$$

$$<i_{rin}^2> = (RGL_1L_2P_s/(MK))^2(RIN)B_e$$

where P_s is the average input optical power of the signal, m is the optical modulation index, P_{ASE} is the power of amplified spontaneous emission noise, R is the responsivity of the photodetector, B_e is the receiver bandwidth, B_O is the bandwidth of the optical filters, L_1 includes the excess loss of coupler 1 and the fiber losses before the EDFAs, and L_2 includes the excess loss of coupler 2 and fiber losses between EDFAs and receiver nodes, k is the Boltzman constant, h is the Plank constant, v is the frequency, T is the temperature and R_e is the effective noise resistance of the receiver. The expression for each noise term will be considered in more detail in Chapter 5.

For a specified value of CNR, the number of channels can be calculated as [14]

$$N = \frac{\mu^2 P^2 C^2}{CNR[<i_{th}^2> + 2qCP + 4n_{sp}hvL_2R(G-1)(PCK + n_{sp}hv(G-1)B_oL_2)/K^2 + C^2P^2RIN]B_e} \tag{3.2}$$

where $C = GRL_1L_2/(MK)$ and $\mu = m\sqrt{N/2}$.

As mentioned earlier in Section 1.3, the total rms modulation index μ can not exceed a certain value when many channels are transmitted because the nonlinear distortion produced by overmodulating the laser diode (clipping distortion occurring when the current to the laser is below threshold) needs to be kept below a specific value. Chung and Jacobs [7] [15] demonstrated from both experiments and simulations that μ should not exceed about 0.3. This will be described further in Section 6.1. Assuming the laser diodes are modulated at this maximum modulation index, there is a maximum number of channels which may be transmitted through the system. This is the capacity of the system in term of the number of channels.

If G is small (~1), the system is shot noise limited and equation (3.2) becomes

$$N = \frac{R P_r \mu^2}{4qB_e(CNR)} \tag{3.3}$$

where Pr is the average received optical power. Then, the channel capacity can be expressed, as reported by Saleh [5] and Minasian and Alameh [16], in terms of the number of channels per milliwatt of the received optical power. If G is sufficiently large and an optical filter is used such that the optical bandwidth is sufficiently small that spontaneous-spontaneous beat noise may be neglected, then the signal-spontaneous noise is the dominant contribution to the noise at the receiver, and equation (3.2) can be approximated as

$$N = \frac{L_1 P_s \mu^2}{4 h\nu n_{sp} B_e(CNR)M} \tag{3.4}$$

Notice that Ps in the numerator is the input signal power. Therefore, in this limit, the product NM is constant. This suggests that for the single-pump configuration, M should be large to maximize capacity, since the capacity is given by N(M-1). (However, the input pump power decreases with increasing M and reduces the capacity.) Also, it implies that for the multiple-pump configuration, the capacity NM, which can be achieved if the population inversion of the EDFAs is complete, is independent of either the number of input ports or the number of output nodes.

However, both the shot noise and signal-spontaneous beat noise are large in the system we are concerned with here. The capacity is no longer simply proportional to the received optical power because it also depends on the characteristics of the EDFAs. The evaluation of the performance thus requires modeling of the gain and spontaneous-emission factor of the EDFAs, which will be described in Chapter 7.

3.2 The Effect of Pump Power on the Capacity

It has been pointed out earlier that the pump power of the single pump configuration sets a limit on the system. Currently, the power of the pump laser is not very large. The pump power at each EDFA of the single-pump configuration may be too small after splitting if the number of input ports of the first-stage star is large. Therefore the number of ports of the first-stage star can not be large and the capacity is strictly limited. The capacity can be increased by increasing the pump power. Figure 3.1 compares the behaviors of the M=4 network with the baseline for the same number of output nodes. These curves are calculated from equation (3.2) using the parameters in Table 2.1 and calculating amplifier gain and noise from the result of modeling which is to be described in Chapter 7. The lengths of the EDFAs are chosen to maximize the gains. The EDFAs are put right after the first star coupler. If the single pump powers exceed certain values, the structure of M=4 begins to show advantages over the baseline. Therefore, whether the baseline or the M=4 network is better depends on the power of the pump laser.

In addition to the magnitude of the pump power affecting the system, the wavelength of the pump light makes a difference too. Currently most EDFAs are pumped either by 1480nm pump lasers or by the 980nm pump lasers. The 980nm pump provides a more complete population inversion, giving a smaller spontaneous emission factor. Both wavelength pumps can be modeled in the same way in our formulation. The results given here are for the 1480nm-pump case, for which more information was available.

3.3 The Relation of the Number of Channels and the Number of Output Nodes

We always wish we can transmit a large number of CATV channels to a huge number of subscribers. However, there is a trade-off between these two numbers. Since the total modulation index can not exceed a certain small value, the modulation index per channel will be too small to provide big enough values of CNR for a large number of output nodes if the number of channels becomes very large.

Similarly, if many subscribers are accommodated, the number of channels to be transmitted can't be very large.

Figure 3.2 is obtained by using the similar calculation as in Figure 3.1. It shows the results of the single-pump configuration. The total number of channels is plotted as a function of the number of output nodes. It is seen that if the number of output nodes is less than 96, more channels may be transmitted through the M=4 structure than through either the baseline case, or the cases of M=2 or 8. Note that the total number of channels may reach 600.

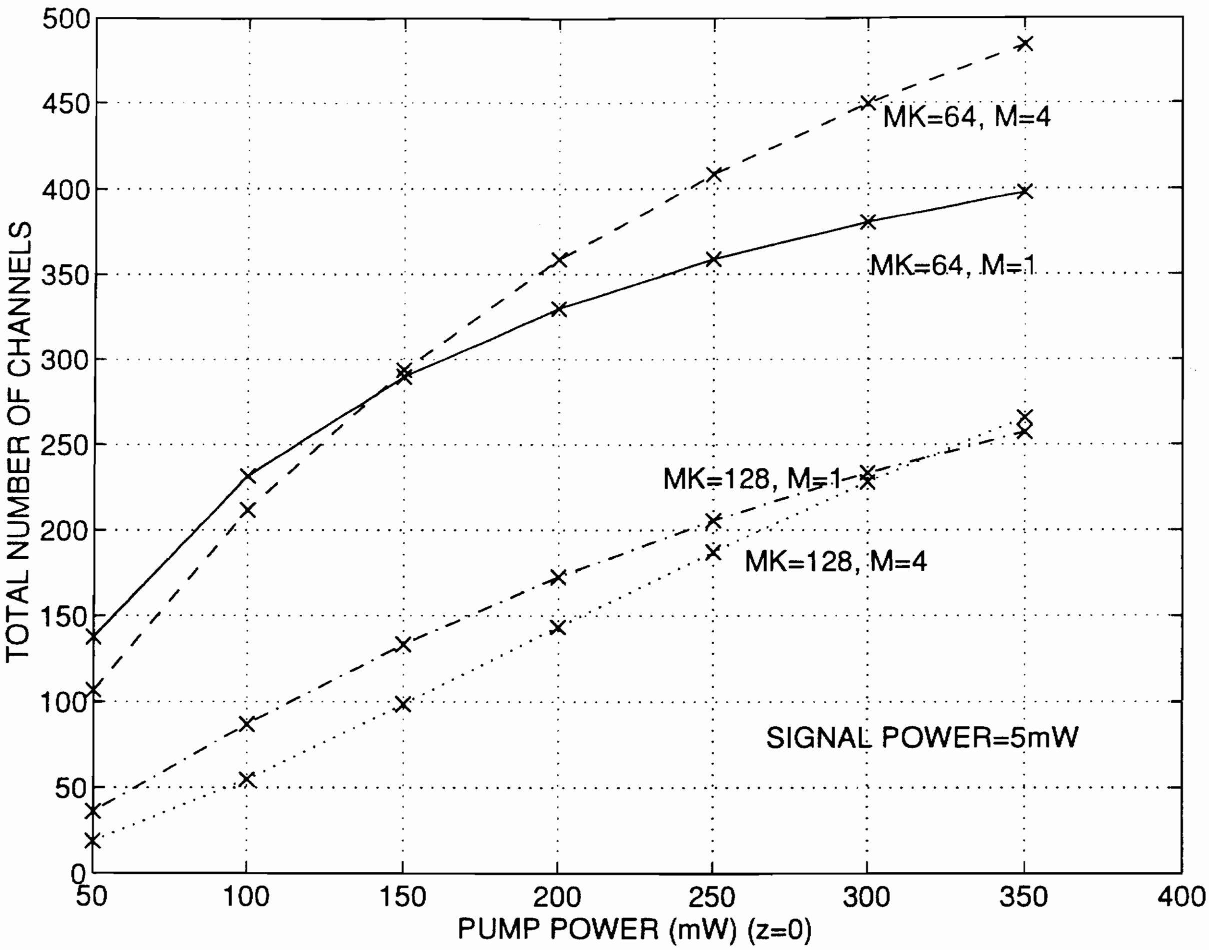

FIGURE 3.1 THE CAPACITIES vs. PUMP POWERS

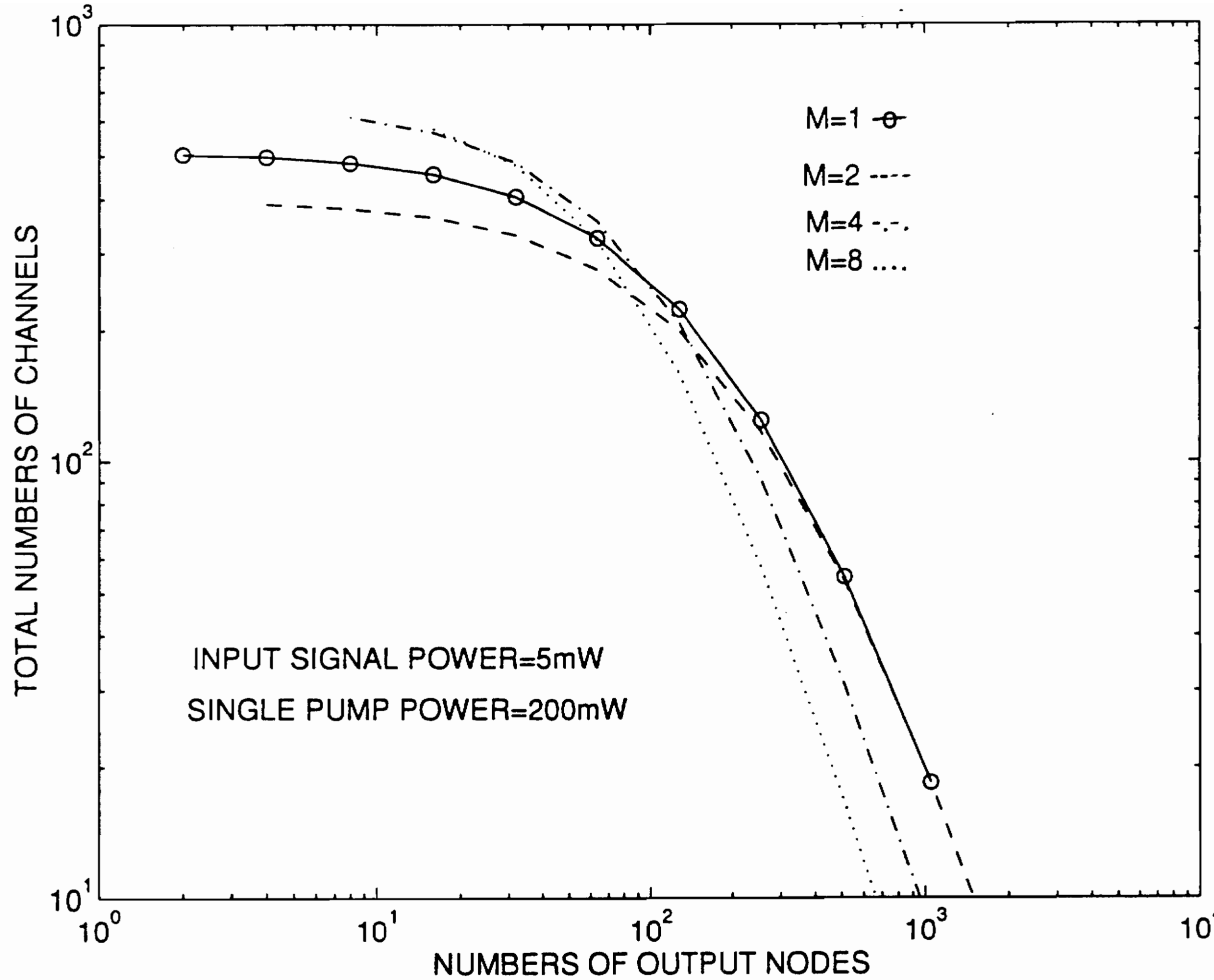

FIG 3.2 TOTAL NUMBERS OF CHANNELS vs. NUMBERS OF OUTPUT NODES

CHAPTER 4 NETWORK PERFORMANCE ANALYSIS

The network performance here refers to the CNR at the receiver and the number of output nodes which may be reached at the same time. The total number of CATV channels is fixed. If the number of output nodes becomes larger, the value of CNR decreases. To assure adequate quality, the CNR at the receiver must be larger than a specified value.

4.1 CNR vs. the Number of Output Nodes

The performance of the network with a single pump laser as a function of the number of output nodes is plotted in Figure 4.1. The results are obtained basically from equation (3.1). When a 4X4 star coupler is used, the number of output nodes reaches 132 with the minimum CNR requirement of 50dB and a total of 200 channels transmitted. When M=8, the value of CNR decreases more rapidly. The curve of M=8 shows fewer output nodes (112) for 50dB CNR. It is seen that the baseline provides better performance than the M=4 network except when fewer than 96 output nodes are needed. This is due to the insufficient pump power, as demonstrated earlier in Figure 3.1.

For the multiple-pump configuration, the system performance for transmitting a total of 200 channels is plotted in Figure 4.2. The length of the EDFA is again chosen to achieve the maximum gain. It is seen that the number of output nodes increases to 322, 572 for the cases of M=2, 4 respectively. The advantage of the two-stage star network is now much greater.

4.2 Optimization of System Performance

The optimum design of CATV distribution systems depends greatly on the characteristics of the laser diodes and pump lasers used. If the power of the pump lasers is very large and the length of EDFA is not long (<Lmax), the two-stage star network with the single-pump configuration may be a good design. If the number of channels required to be transmitted is relatively small, the baseline, which has only one 1XK splitter may be the best choice.

There is an optimal position of the EDFA, (between the first-stage and second-stage star couplers) at which the highest CNR or the largest channel capacity may be achieved. For the distribution distance of 10km, the optimum position is right after the first-stage star. This is shown by plotting the number of channels accommodated as a function of the position of the EDFA (calculated from equation (3.2)) in Figure 4.3. The values on the X axis represent the normalized distance, which is the distance between the EDFA and the first-stage star divided by the fiber length between two star couplers. For example, z=0 corresponds to the position right after the first-stage star and z=1 corresponds to that right before the second-stage star. It is seen that the number of channels decreases when the EDFA is moved closer to the receiving end. The optimum position may change if the distribution distance is greater than 20km. For such cases the power at the output of the first coupler must be large, in which case the amplifier would saturate if it were at this output.

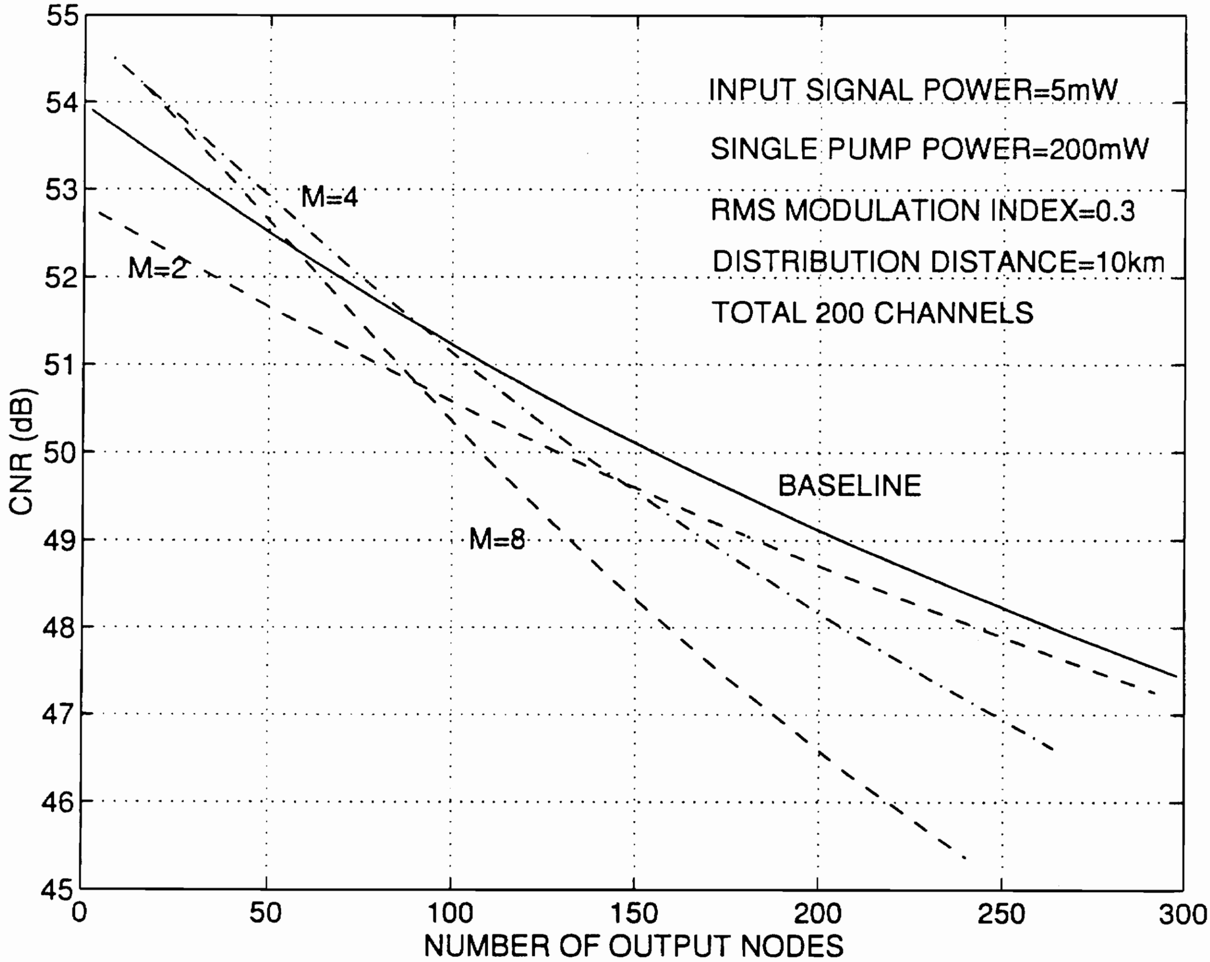

FIGURE 4.1 COMPARISON OF SIGNLE-PUMP NETWORK WITH BASELINE

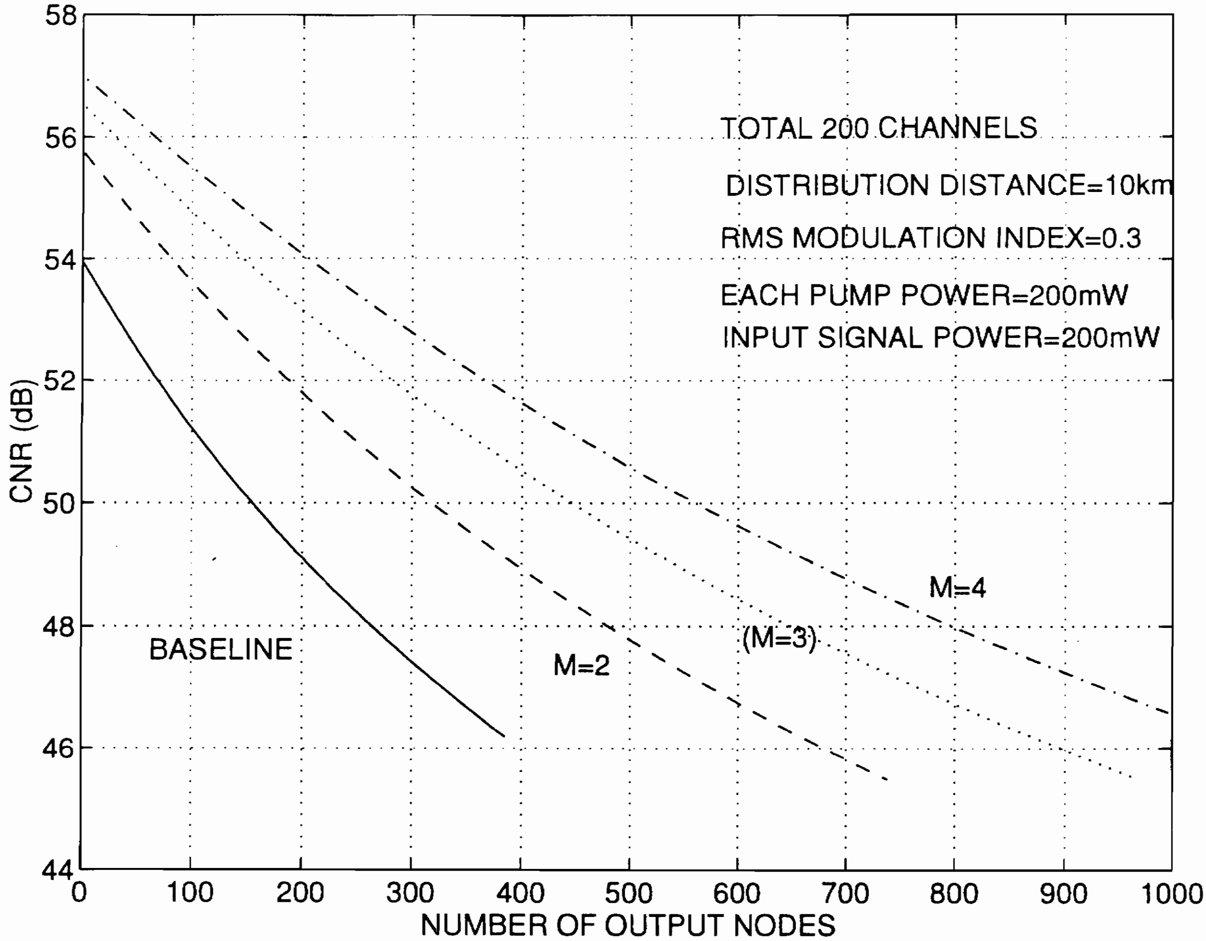

FIGURE 4.2 COMPARISON OF MULTIPLE-PUMP NETWORK WITH BASELINE

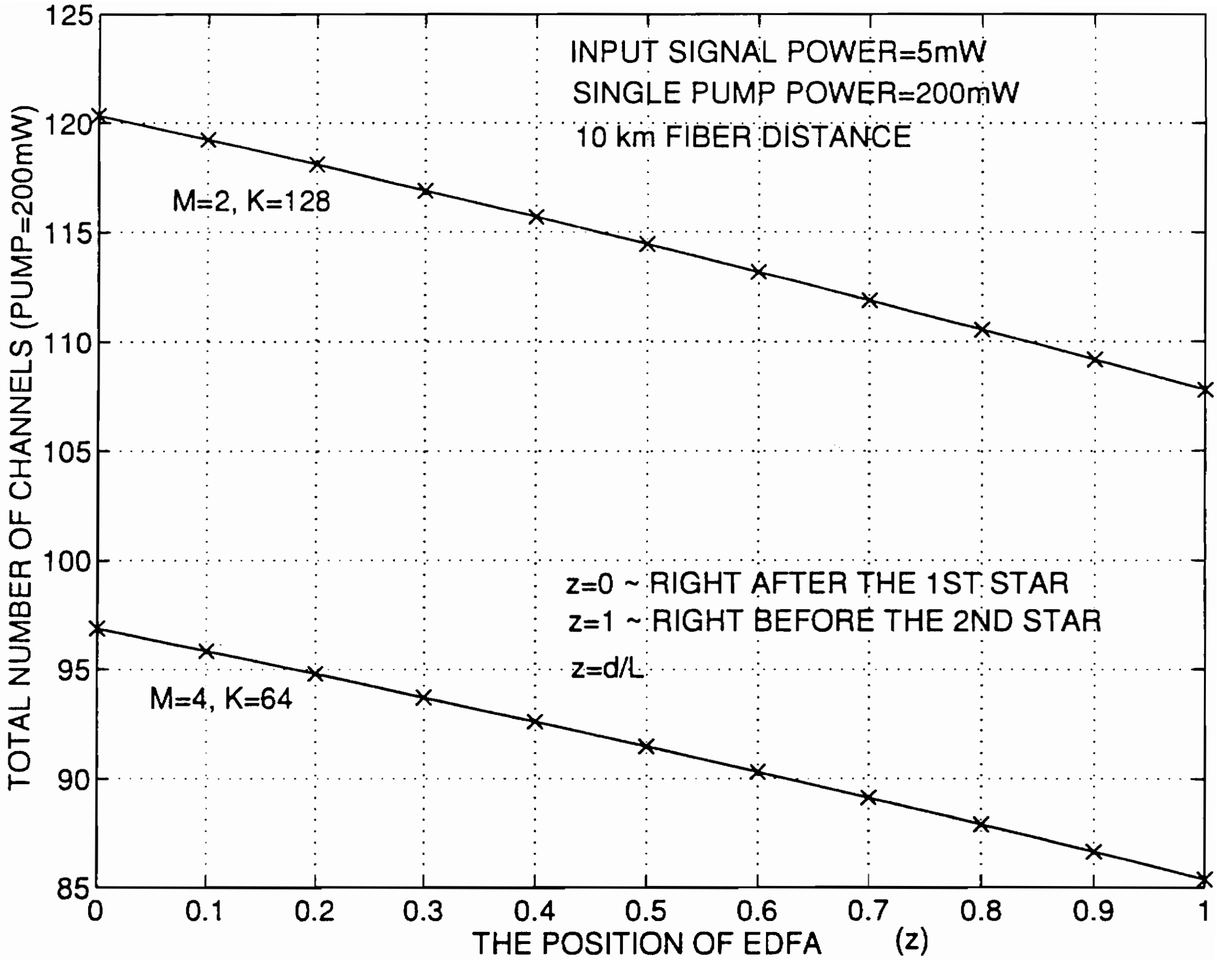

FIGURE 4.3 THE CAPACITIES vs. POSITION OF EDFA

PART B NOISE, DISTORTION AND MODELING

CHAPTER 5 NOISE IN THE SYSTEM

The capacity and performance of the system have been analyzed in Part A by numerical evaluation of the noise impairment. It is important to investigate the physics of the noise so that the approaches to reduce the noise impairment may be found. This chapter covers the laser RIN, the reflection induced noise and the optical amplifier noise as well as the enhancement of noise due to their combined effect. A discrepancy in the published results on the laser RIN is pointed out. Reflection induced noise is investigated and it is shown that only doubly reflected terms need be considered. Reflection induced noise may be increased when an optical amplifier is used, although it is small compared with ASE noise and shot noise if the reflections are kept sufficiently low.

5.1 Laser Relative Intensity Noise:

In AM-SCM CATV system, the optical output is relatively large and then the relative intensity noise (RIN) is an important degradation and sets a limit on the system. The intrinsic RIN of lasers in fiber optic communications is investigated in this chapter. The other form of RIN caused by multiple reflections will be investigated in Section 5.2. It is shown that RIN is proportional to the inverse square of the output optical power and it is also related to the threshold current of the laser when the modulating signal is large. This result raises a question on some published results.

5.1.1. The expressions for RIN:

Due to spontaneous emission and electron-hole recombination, the output of a semiconductor laser exhibits fluctuations in intensity, phase and frequency. We can study this laser noise by adding a Langevin noise source to the single-mode rate equations, as follows: [17]

$$\frac{dN}{dt} = -\gamma(N - N_T)S + \frac{I\Gamma_e}{qV} - \frac{N}{\tau_c} + F_N(t) \tag{5.1}$$

$$\frac{dS}{dt} = -\Gamma\gamma(N - N_T)S - \frac{S}{\tau_p} + \frac{\Gamma\beta N}{\tau_c} + F_s(t) \tag{5.2}$$

$$\frac{d\phi}{dt} = \frac{1}{2}\beta_c(\gamma(N - N_T) - \frac{1}{\tau_p}) + F_\phi(t) \tag{5.3}$$

where N and S are electron density and photon density, N_T is the transparency electron concentration, Γ and Γe are the light confinement factor and the electron confinement factor. τ_p, τ_c are the photon lifetime and electron lifetime respectively. γ is the differential gain coefficient. ϕ is the phase of the output light. I is the injected current, β_c is the amplitude-phase coupling parameter, commonly called the linewidth enhancement factor. Typical values of β_c for InGaAsP lasers are in the range 4-8, depending on the operating wavelength. $F_N(t)$, $Fs(t)$ and $F\phi(t)$ are the Langevin forces. V is the volume of the laser, and q is the electron charge.

The RIN is defined as

$$RIN = S_P(\omega)/P^2 \tag{5.4}$$

where the spectral density $S_P(\omega)$ is given by

$$S_P(\omega) = \int_{-\infty}^{\infty} <\delta S(t+\tau)\delta S(t)> \exp(-i\omega\tau)d\tau \tag{5.5}$$

From equation (5.1-5.3) the following expression is obtained [17-19]:

$$RIN(\omega) = \frac{2 n_{sp}[\omega^2 + (\gamma S_0)^2 \frac{N\tau_p}{\tau_c n_{sp} S_0} + \frac{1}{\tau_c^2}]}{VS_0\tau_p[(\Omega_R - \omega)^2 + \Gamma_R^2][(\Omega_R + \omega)^2 + \Gamma_R^2]} \tag{5.6}$$

where $\Gamma_R = \frac{1}{2}(\frac{1}{\tau_c} + \gamma S_0 + \frac{n_{sp}}{\tau_p V S_0})$, $\Omega_R \approx (\gamma S_0 / \tau_p)^{1/2}$. RIN($\omega$), as calculated from equation (5.6), is plotted as a function of ω in Figure 5.1, for a representative choice of laser parameters, as given in Table 5.1.

We see from Figure 5.1 that the magnitude of RIN is constant over a wide range of ω, and has a peak only in the vicinity of Ω_R. The behavior of the RIN in the vicinity of Ω_R, is shown for various Po in Figure 5.2. In practical systems, we are concerned with RIN(0), which from (5.6) is given by

$$RIN(0) = \frac{2 n_{sp}[(\gamma S_0)^2 \frac{N\tau_p}{\tau_c n_{sp} S_0} + \frac{1}{\tau_c^2}]}{V S_0 \tau_p [\Omega_R^2 + \Gamma_R^2]^2} \tag{5.7}$$

Since $\Gamma_R \ll \Omega_R$, $\Omega_R = (\gamma S_0 / \tau_p)^{1/2}$, (5.7) becomes

$$RIN(0) = \frac{2 n_{sp} \tau_p [(\gamma S_0)^2 \frac{N\tau_p}{\tau_c n_{sp} S_0} + \frac{1}{\tau_c^2}]}{V S_0^3 \gamma^2} \tag{5.8}$$

5.1.2 The behavior of laser RIN on the output optical power:

In the steady state

$$S_0 = \frac{\Gamma \Gamma_e \tau_p}{qV}(I - I_{th})$$
$$N_{th} = \frac{\Gamma_e \tau_c I_{th}}{qV}$$

Then we can express RIN in terms of $I - I_{th}$, which is proportional to the output optical power, as

$$P_{fiber} = C_1 C_2 \eta_d \frac{hc}{q\lambda}(I - I_{th}),$$

$$\mathrm{RIN}(0)=\frac{2n_{sp}[(\frac{\gamma\Gamma\Gamma_e\tau_p}{qV})^2\frac{(I-I_{th})I_{th}}{\Gamma n_{sp}}+\frac{1}{\tau_c{}^2}]}{V(\frac{\Gamma\Gamma_e}{qV})^3\tau_p{}^2\gamma^2(I-I_{th})^3} \tag{5.9}$$

When the laser is modulated with large signals, $I-I_{th}>10^{-2}$ A, the above equation can be simplified to

$$\mathrm{RIN}(0)=\frac{2I_{th}q}{\Gamma^2\Gamma_e}\frac{1}{(I-I_{th})^2} \tag{5.10}$$

while, with small signals, (5.9) leads to the expression

$$\mathrm{RIN}(0)=\frac{2n_{sp}}{V(\frac{\Gamma\Gamma}{qV})^3\gamma^2\tau_c{}^2\tau_p{}^2}\frac{1}{(I-I_{th})^3} \tag{5.11}$$

The expressions (5.9-5.11) are plotted in Figure 5.3. The figure shows that when $I\text{-}I_{th}$ is small equation (5.11) is a good approximation, meaning RIN is inversely proportional to the cube of output optical power , and when $I\text{-}I_{th}$ gets larger, RIN(0) becomes proportional to the inverse square of output optical power. This large-signal behavior differs from the statement made in [18-20] that RIN(0) is proportional to the reciprocal of the optical power. This might be a result of laser parameters degrading as P is increased. An interesting consequence of equation (5.10) is that laser RIN is inversely proportional to $(I\text{-}I_{th})^2$ but proportional to I_{th}. Contours of constant RIN(0), are shown as a function of power coupled into the fiber and I_{th} in Figure 5.4. Figure 5.5 shows a three-dimensional plot of RIN(0) as a function of I_{th} and $I\text{-}I_{th}$. It is seen that the smaller I_{th} and the larger $I\text{-}I_{th}$, the smaller is the RIN. Thus, for a given optical power, RIN is reduced if I_{th} is reduced. From some equations in [18], we obtain

$$I_{th}=\frac{qLwd}{\tau_c\Gamma_e}\left(\frac{v_g[\alpha_{int}+\frac{1}{2L}\ln(\frac{1}{R_1R_2})]}{\gamma}+N_T\right), \tag{5.12}$$

where L, w and d are the length, width and thickness of the active region of laser, and v_g is the group velocity, α_{int} the internal loss coefficient, R the reflectivity. So if we can reduce the size of the active region, specifically the width and the thickness, smaller I_{th} may be achieved. This is being done with multiple quantum well (MQW) lasers.

5.1.3 The RIN noise performance:

The value of laser intrinsic RIN has been reduced significantly with the development of laser technology. Special lasers developed for analog application can achieve RIN of less than -160 dB/Hz, at which the RIN will not be the dominant noise in the CATV distribution network. With the representative parameters used in our modeling, RIN is taken to be -155dB/Hz.

5.2 *Reflection Induced Noise*

In fiber optic communication systems, there exist many refractive index discontinuities occurring at splices, connectors and fiber ends. Some light is reflected and bounces back and forth, generating additional intensity noise. In this section, reflection induced noise is analyzed. In addition to summarizing the previous literature, the polarization and higher order reflections are taken into account in the analysis.

5.2.1 Two reflection interfaces:

Two discontinuities in a fiber transmission line form a Fabry-Perot interferometer, as shown in Figure 5.6. The characteristics of the interferometer are determined by the intensity reflection coefficients R_1 and R_2, the round trip delay time τ, and the single pass intensity transmittance α. The delay time τ is the time the doubly reflected light takes to travel back to the same output point. Assuming that the laser is operating under continuous wave condition and the output light has linear polarization, the optical field into the interferometer can be described as

$$\vec{e}_i(t) = \vec{P}_i E_0 \cos(\omega_0 t + \varphi(t)) \qquad (5.13)$$

where E_0 is the field amplitude, ω_0 is the laser center frequency, $\phi(t)$ is the random phase which contains all deviations from a monochromatic wave and $\vec{P}_i$ is the polarization vector.

In previous literature, the doubly reflected field was considered. In addition to the doubly reflected field, we consider here the quadruply reflected field. Terms of order $(R_1R_2)^{3/2}$ and higher are neglected, since the reflection coefficients are generally small. Then the output of the interferometer may be approximated as the combination of the following fields:

$$\vec{e}(t) = E_0(1-R_1)^{1/2}(1-R_2)^{1/2}[\alpha^{1/2}\vec{e}_i(t) + \alpha^{3/2}(R_1R_2)^{1/2}\vec{e}_i(t-\tau) + \alpha^{5/2}R_1R_2\vec{e}_i(t-2\tau)] \qquad (5.14)$$

where α is the transmittance of the fiber. The intensity of the output light I(t) can be written as [21]

$$I(t) = |\vec{e}(t)|^2 = \alpha E_0^2(1-R_1)(1-R_2)[1+\rho(t,\tau)] \qquad (5.15)$$

where

$$\rho(t,\tau) = 2R\beta_P\cos(\omega_0\tau + \phi(t,\tau)) + \beta_P R^2[1 + 2\cos(2\omega_0\tau + \phi(t,2\tau))] \qquad (5.16)$$

Here the effective reflection coefficient R equals $\alpha\sqrt{R_1R_2}$. We have ignored the terms of higher order in R, and β_P is a parameter, less than one, dependent on the difference of polarization of the direct and doubly reflected signals. The phase terms are given by $\phi(t,\tau) = \varphi(t) - \varphi(t-\tau)$ and $\phi(t,2\tau) = \varphi(t) - \varphi(t-2\tau)$.

5.2.2 Laser phase behavior

Due to the dynamic characteristics of the laser process, the phase of the output light keeps changing. The phase of the field is assumed to undergo a Wiener-Levy random process, which is a non-stationary zero-mean Gaussian random process. This model gives an autocorrelation function for the phase fluctuations as

$$<\varphi(t_1)\varphi(t_2)>=\kappa\min(t_1,t_2)$$

where t_1 and t_2 are two arbitrary time instants, $\min(t_1, t_2)$ equals the smaller of t_1 and t_2, and κ is a constant determined by the characteristics of the physical process being considered. From this model, we can find that the difference of two phases is also a zero-mean Gaussian variable with a variance [22]

$$\sigma^2(t_1-t_2)=\kappa|t_1-t_2|$$

$1/\kappa$ is called the coherence time of the laser. If the full width half maximum (FWHM) linewidth of the laser is denoted by Δv, κ is found to be $2\pi\Delta v$.

5.2.3 Power spectral density of reflection induced noise

The fluctuations of the phase differences are converted into the intensity fluctuations called relative intensity noise, as implied in equation (5.15). The noise spectral density can be calculated from the Fourier transform of the autocorrelation function of $\rho(t,\tau)$:

$$<\rho(t_1,\tau)\rho(t_1+t,\tau)>/\beta_p^2$$

$$=E[2R^2\cos(\phi(t_1,\tau)-\phi(t_1+t,\tau))+2R^2\cos(2\omega_0\tau+\phi(t_1,2\tau)+\phi(t_1+t,\tau))$$

$$2R^3\cos(\omega_0\tau+\phi(t_1,\tau))+2R^3\cos(\omega_0\tau+\phi(t_1+t,\tau))$$

$$2R^3\cos(3\omega_0\tau+\phi(t_1,\tau)+\phi(t_1+t,2\tau))+2R^3\cos(\omega_0\tau+\phi(t_1+t,2\tau)-\phi(t_1,2\tau))] \quad (5.17).$$

Using $E[\exp(j(\varphi(t_1)-\varphi(t_2))]=\exp(-\sigma^2(t_1-t_2)/2)$, the above autocorrelation function can be evaluated and the result consists of four terms:

$$<\rho(t_1,\tau)\rho(t_1+t,\tau)>/\beta_p^2=F_1+F_2+F_3+F_4 \quad (5.18)$$

where

$$F_1 = 2R^2 \begin{cases} \exp(-2\pi\Delta v|t|)[1+\cos(2\omega_0\tau)\exp(-4\pi\Delta v(\tau-|t|))], & |t|<\tau \\ \exp(-2\pi\Delta v\tau)[1+\cos(2\omega_0\tau)], & |t|>\tau \end{cases}$$

$$F_2 = 2R^3 \begin{cases} \exp(-5\pi\Delta v|t|)\cos(3\omega_0\tau)+\exp(-\pi\Delta v\tau)\cos(\omega_0\tau), & |t|<\tau \\ \exp(-\pi\Delta v(7\tau+2|t|))\cos(3\omega_0\tau)+\exp(-2\pi\Delta v|t|+\pi\Delta v\tau)\cos(\omega_0\tau), & \tau<|t|<2\tau \\ \exp(-3\pi\Delta v\tau)[\cos(3\omega_0\tau)+\cos(\omega_0\tau)], & |t|>2\tau \end{cases}$$

$$F_3 = 4R^3\exp(-\pi\Delta v\tau)\cos(\omega_0\tau)$$

$$F_4 = 2R^3 \begin{cases} \exp(-5\pi\Delta v\tau+2\pi\Delta v|t|)\cos(3\omega_0\tau)+\exp(-2\pi\Delta v|t|-\pi\Delta v\tau)\cos(\omega_0\tau), & |t|<\tau \\ \exp(-3\pi\Delta v\tau)[\cos(3\omega_0\tau)+\cos(\omega_0\tau)], & |t|>\tau \end{cases}$$

The Fourier transform of the autocorrelation function gives the power spectral density of RIN. The Fourier transform of F1 is

$$\begin{aligned} &\int_{-\infty}^{\infty} F_1\exp(-j2\pi ft)dt \\ &= \exp(-2\pi\Delta v\tau)[1+\cos(2\omega_0\tau)](\delta(f)-\sin(2\pi f\tau)/\pi f) \\ &+\frac{1}{\pi}\frac{\Delta v}{f^2+\Delta v^2}[1-\exp(-2\pi\Delta v\tau)(\cos(2\pi f\tau)+\frac{f}{\Delta v}\sin(2\pi f\tau))] \\ &\quad -\frac{\cos(2\omega_0\tau)}{\pi}\frac{\Delta v}{f^2+\Delta v^2}\exp(-4\pi\Delta v\tau)[1-\exp(2\pi\Delta v\tau)(\cos(2\pi f\tau)-\frac{f}{\Delta v}\sin(2\pi f\tau))] \end{aligned} \tag{5.19}$$

Similarly, the Fourier transform of the other terms can be obtained. But the simpler expressions at the coherent and incoherent extremes are of more concern than the long and complicated general expression. Therefore, the whole Fourier transform of $<\rho(t_1,\tau)\rho(t_1+t,\tau)>$ is not given here.

In practice, the distance between the reflection points is longer than 1 meter. For example, for a 3m fiber jumper, the round trip delay time is about 30ns. If the linewidth Δv is 40MHz, then $2\pi\Delta v\tau$ equals 7.5 (considered much larger than 1). Since the incoherent case, with $2\pi\Delta v\tau >> 1$, is encountered in practice, the value of RIN(f) at this limit is of most concern. It can be written as

$$\mathrm{RIN}(f) = 4 <\beta_P{}^2> R^2 \frac{1}{\pi}\frac{\Delta v}{f^2+\Delta v^2} + 4 <\beta_P{}^2> R^3 \frac{\cos\omega_0\tau}{\pi}\frac{\Delta v}{f^2+\Delta v^2}\exp(-\pi\Delta v\tau) \quad (5.20)$$

It is seen that there is a exponential factor in the second term including R^3. In the incoherent case, $\exp(-\pi\Delta v\tau) \to 0$ so that the second term can be neglected. Then

$$\mathrm{RIN}(f) = 4 <\beta_P{}^2> R^2 \frac{1}{\pi}\frac{\Delta v}{f^2+\Delta v^2} \quad (5.21)$$

5.2.4 Polarization factor

Now let's consider the value of polarization factor $<\beta_P{}^2>$. It is known that if the polarizations of two fields are parallel then the total intensity is four times the individual intensity, and, if perpendicular then twice, as shown in Figure 5.7. Assuming for simplicity that the polarization direction is uniformly distributed in angle, then the average polarization factor should be

$$<\beta_P{}^2> = \frac{4}{\pi}\int_0^{\pi/4}\cos^2\theta d\theta = \frac{1}{2}+\frac{1}{\pi} \approx 0.82 \quad (5.22)$$

Substituting this value into equation (5.20), we obtain the expression for RIN, and the result is plotted in Figure 5.8. It is seen from the plot that RIN is larger in the low frequency region than in the high frequency region. The difference between RIN at DC and 1GHz is as large as 10dB/Hz.

To summarize, the reflection induced noise contributed by the quadruply reflected field is negligible in the incoherent case. Also, the noise is actually reduced by a factor of 0.18 due to the change of the polarization of the reflected field.

5.3 Optical Amplifier Noise

As indicated in Part A, optical amplifiers may be used in lightwave CATV distribution networks to improve the system performance by overcoming the distribution losses. (including attenuation, splitting losses and excess losses). However, the optical amplifier introduces additional noise to the system. As a result, this amplifier noise could be the ultimate limiting factor for system applications. Thus, in this section we will summarize the various contributions of optical amplifier noise to the noise at the output of the electrical receivers.

The noise is caused by spontaneous emission in the amplifier. The spectral power density of amplified spontaneous emission (ASE) noise is

$$S(f) = 2\, n_{sp} hf (G-1) \tag{5.23}$$

where n_{sp} is greater than 1 but is close to 1 for amplifiers with complete population inversion, and the factor of 2 is due to two polarization directions [12]. For a two-level system, $n_{sp}=N_2/(N_2-N_1)$, where N_2 is the carrier density at the upper level and N_1 at the lower level.

It is found that the receiver noise due to amplifiers results from the beating of spontaneous emission noise with the signal, and the spontaneous and spontaneous as well as RIN and spontaneous beating. The spontaneous emission radiation mixes coherently with the amplified signal at the photodetector and produces a heterodyne component of the photocurrent. The variance of the photocurrent (noise) can be written as

$$\sigma^2 = \sigma_{sh}^2 + \sigma_{th}^2 + \sigma_{RIN}^2 + \sigma_{s-sp}^2 + \sigma_{sp-sp}^2 + \sigma_{RIN-sp}^2 \quad (5.24)$$

where the first three terms are shot noise, thermal noise and relative intensity noise. The last three terms are respectively [12]

signal-spontaneous beat noise, $\sigma^2{}_{s-sp} = 2 I_s I_{ASE} B_e / B_o$ (5.25)

spontaneous-spontaneous beat noise, $\sigma^2{}_{sp-sp} = (I_{ASE})^2 B_e / B_o$ (5.26)

and RIN-spontaneous beat noise $\sigma^2{}_{RIN-sp} = \frac{1}{4}(RIN) I_s I_{ASE} B_e$ (5.27)

Be and Bo are the receiver bandwidth and optical bandwidth; I_S and I_{ASE} are the signal photocurrent and the spontaneous emission photocurrent, $I_{ASE} = RS(f)B_o$ where R is the responsivity of the photodetector.

The amplifier noise figure Fn is often used to specify the amplifier noise performance. However, it has been demonstrated by Jacobs [12] that this may not be an appropriate way because of the difference between the optical measurement and electrical measurement. In our modeling as will be described later, all of the spontaneous emission noise terms are calculated to obtain the value of CNR using the above equations instead of using the noise figure. It is shown that shot noise and signal spontaneous beat noise are the main source of noise in our CATV system.

The above equations may be also used to evaluate the sensitivity of a receiver for digital transmission. Although systems in Part A utilized analog transmission, for completeness we present the sensitivity expressions for digital transmission in an Appendix.

5.4 Noise Enhancement Effects

Although the optical amplifier should provide the system with improvements of capacity and performance, under some conditions it may enhance the noise and degrade the system performance. This section introduces two enhancements on reflection induced noise and spontaneous emission noise. It turns out that the use of amplifiers requires the reflection in the fiber to be very small.

5.4.1 Enhancement of reflection induced noise due to the amplification

In section 5.2, we have analyzed the reflection induced noise which is the intensity noise converted from the phase noise. After the amplifier is employed, the doubly reflected light could go through the amplifier and get amplified again, which is shown in Figure 5.9. The result is that the induced noise is amplified although the reflection coefficient is small. This effect makes the degradation due to the reflection induced noise more severe.

In the incoherent case with $2\pi\Delta v\tau >> 1$, we know from section 5.2 that

$$\mathrm{RIN}(f) = 4 < \beta_P^2 > R^2 \frac{G_1 G_2}{\pi} \frac{\Delta v}{f^2 + \Delta v^2} \tag{5.28}$$

where G_1 and G_2 are the forward gain and backward gain. They are the same if forward and reverse pumping are used, but differ if a single (forward or reverse) pump is used. Consequently the power spectral density of RIN is enlarged by $10\log(G_1G_2)$ dB. For example, if the gain of the amplifier is 20dB, then RIN is enhanced by 40dB. This could contribute to a severe degradation. For example, if the carrier frequency is 1GHz, the linewidth of the laser output is 40MHz and the product of G_1 and G_2 is 30dB, then RIN(f) is about $0.8R^2$. This means that if RIN(f) is required to be below -150dB, R should be less than -75dB. This is a very strict requirement.

5.4.2 Enhancement of spontaneous emission noise due to the reflection

Spontaneous emission radiation propagates in any direction. The spontaneous emission power coming out at both ends are assumed to be the same. Some of the spontaneous emission is reflected back to the EDFA and is amplified again. The total effective ASE power at the output end is [23]:

$$P_{ASE}' = P_{ASE} + R_1G_1P_{ASE} + R_2G_2R_1G_1P_{ASE} + R_1G_1R_2G_2R_1G_1P_{ASE} + \ldots$$

$$= kP_{ASE}, \qquad \text{where } k = \frac{(1 + R_1G_1)}{(1 - R_1R_2G_1G_2)} \tag{5.29}$$

where R_1 is the reflection coefficient before the amplifier and R_2 is the one after. As implied in the above equation, they play different roles for the enhanced ASE power. In the previous section, the effective coefficient R was used because only the product of R_1 and R_2 occurs. With the gain of 20dB, R_1, R_2 should be each less than -30dB so that the ASE power won't be enhanced by more than 10%.

5.4.3 Reducing the reflections

Since the reflection through the amplifier enhances the noise degradation, especially the reflection induced noise, it is essential that all steps are taken to minimize reflections in the amplifier. Reflections can arise by various means, some of which are [24]:

* unterminated fiber ends
* the facets of the pump laser
* poor fusion splices
* connectors
* the reflectance of any dielectric stack type filters.

Reducing their reflections requires avoiding geometrical discontinuities and optical discontinuities at the interfaces.

TABLE 5.1 Typical Values of the Parameters:

SYMBOLS	PARAMETERS	TYPICAL VALUES
τ_p	Photon lifetime	1.4ps
τ_c	Carrier lifetime at threshold	3 ns
N_{th}	Threshold carrier density	$1.5(10)^{18}cm^{-3}$
N_T	Transparency electron concentration	$1.2(10)^{18}cm^{-3}$
S	Photon density in active region	$3(10)^{14}cm^{-3}$
V	Volume of laser active region	$1.8(10)^{-10}cm^3$
I_{th}	Threshold current	20mA
γ	Differential gain coefficient	$2(10)^{-6}cm^3/s$
η_d	External quantum efficiency	0.49
η_{int}	Internal quantum efficiency	1.0
Γ	Light confinement factor	1.0
Γ_e	Carrier confinement factor	0.7
n_{sp}	Spontaneous emission factor	2
q	Electron Charge	$1.6(10)^{-19}c$

N_p	Photon number at the receiver	—
C_e	Effective capacitance	—
V_T	Thermal voltage	0.026ev
I_p	Photo current at the receiver	—
B	Transmission bit rate	1GHz
B_e	Receiver bandwidth	0.7GHz

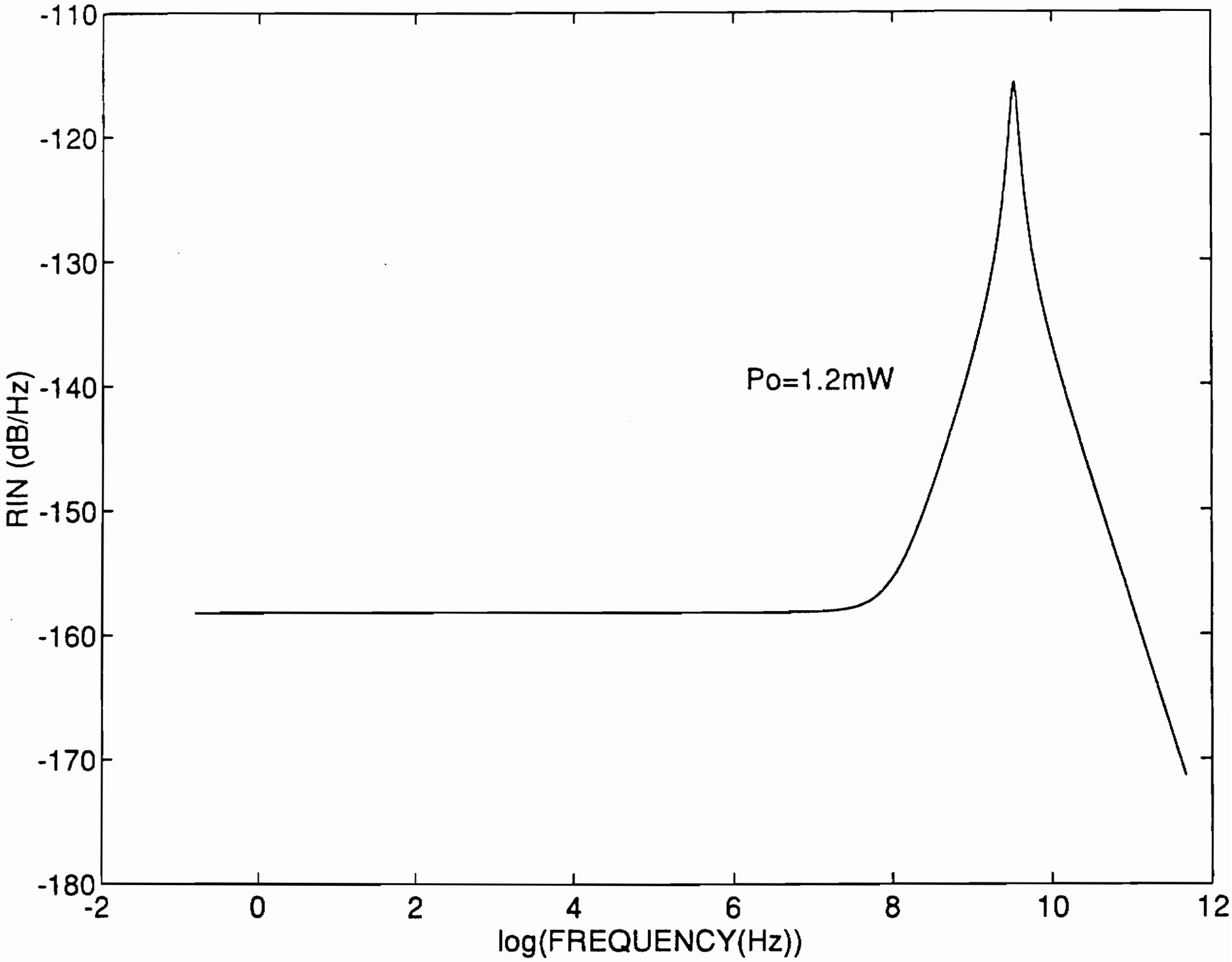

FIGURE 5.1 LASER RELATIVE INTENSITY NOISE

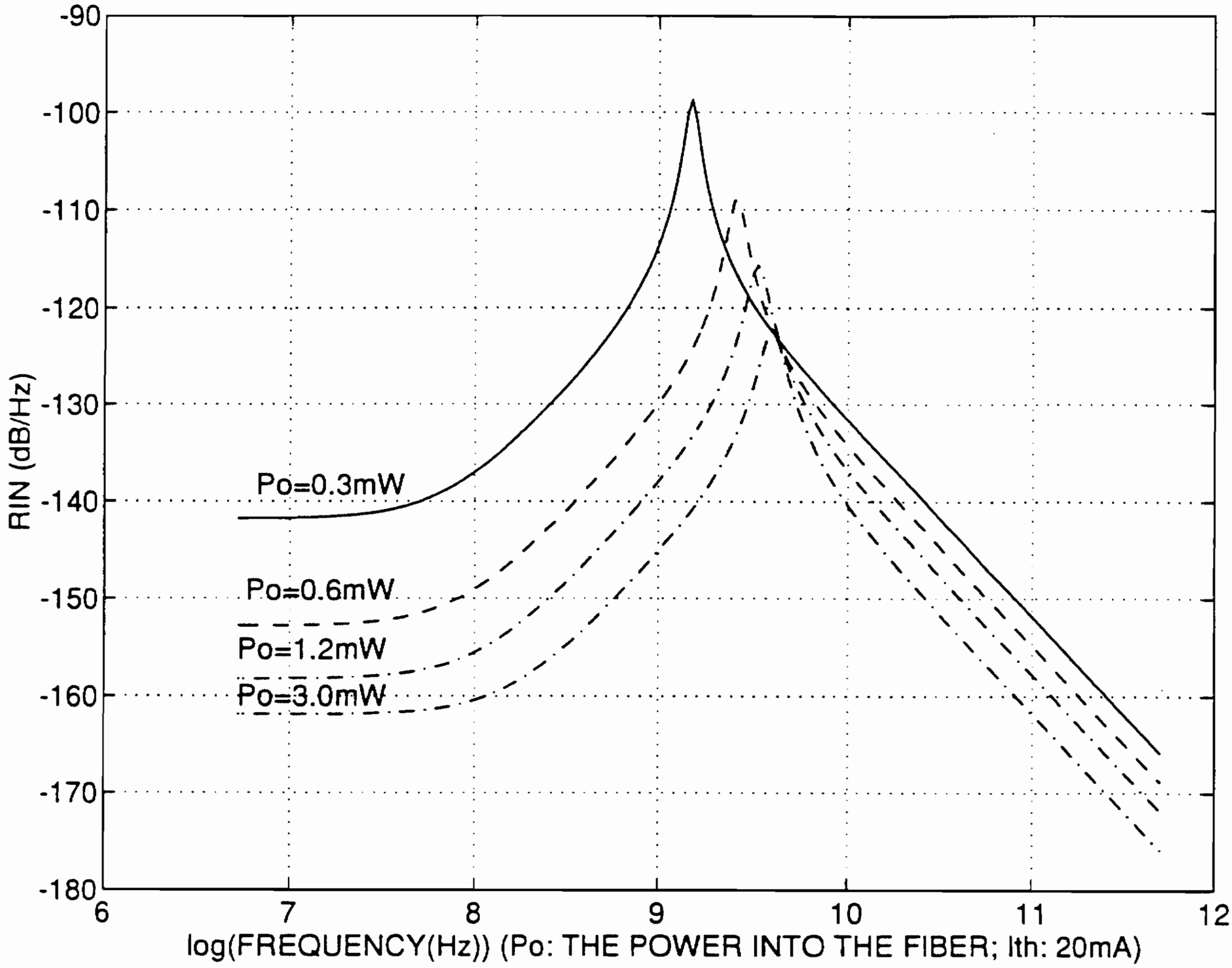

FIGURE 5.2 RIN(f) AT THE VICINITY OF RELAXATION FREQUENCY

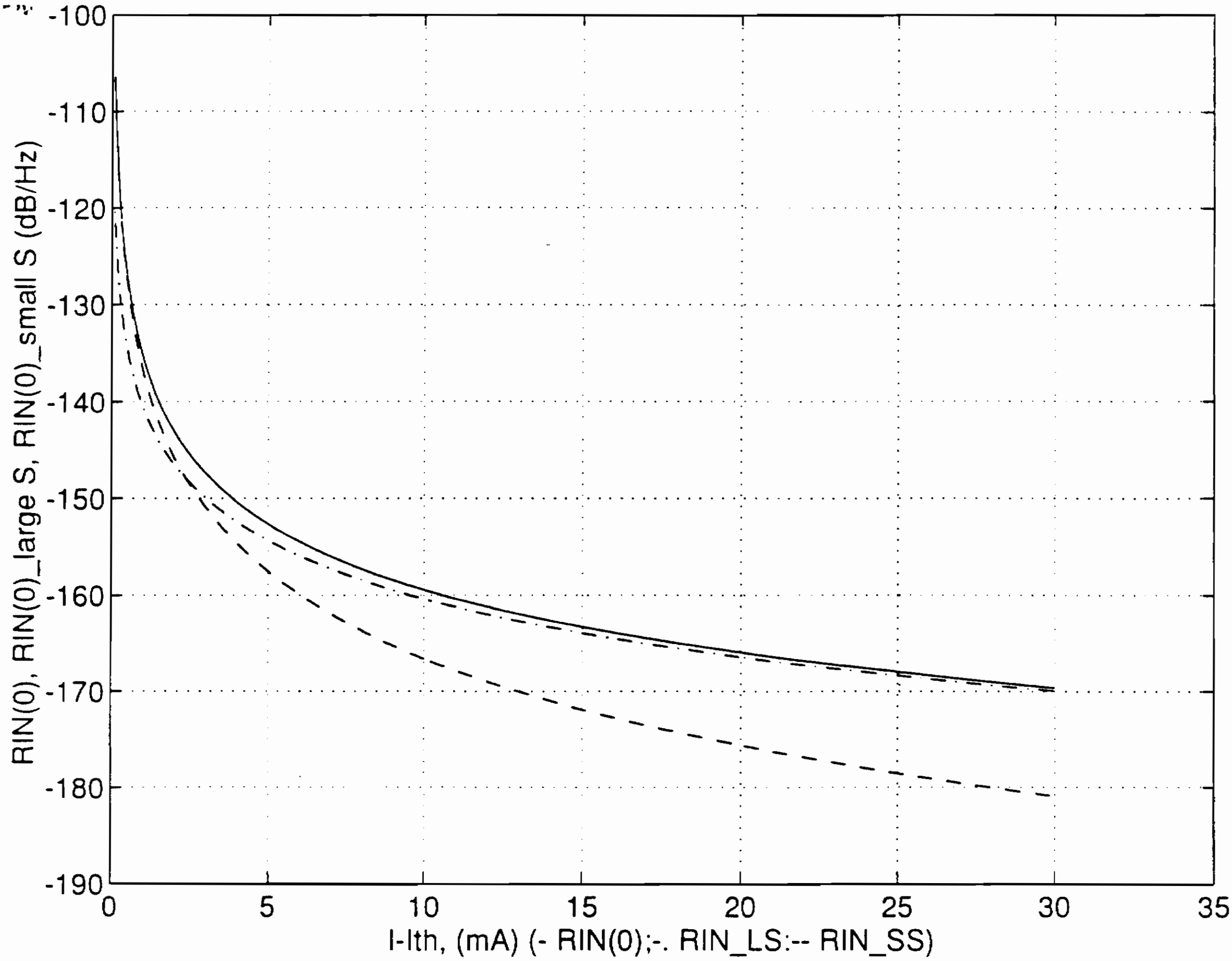

FIGURE 5.3 RIN(0) vs. I-Ith

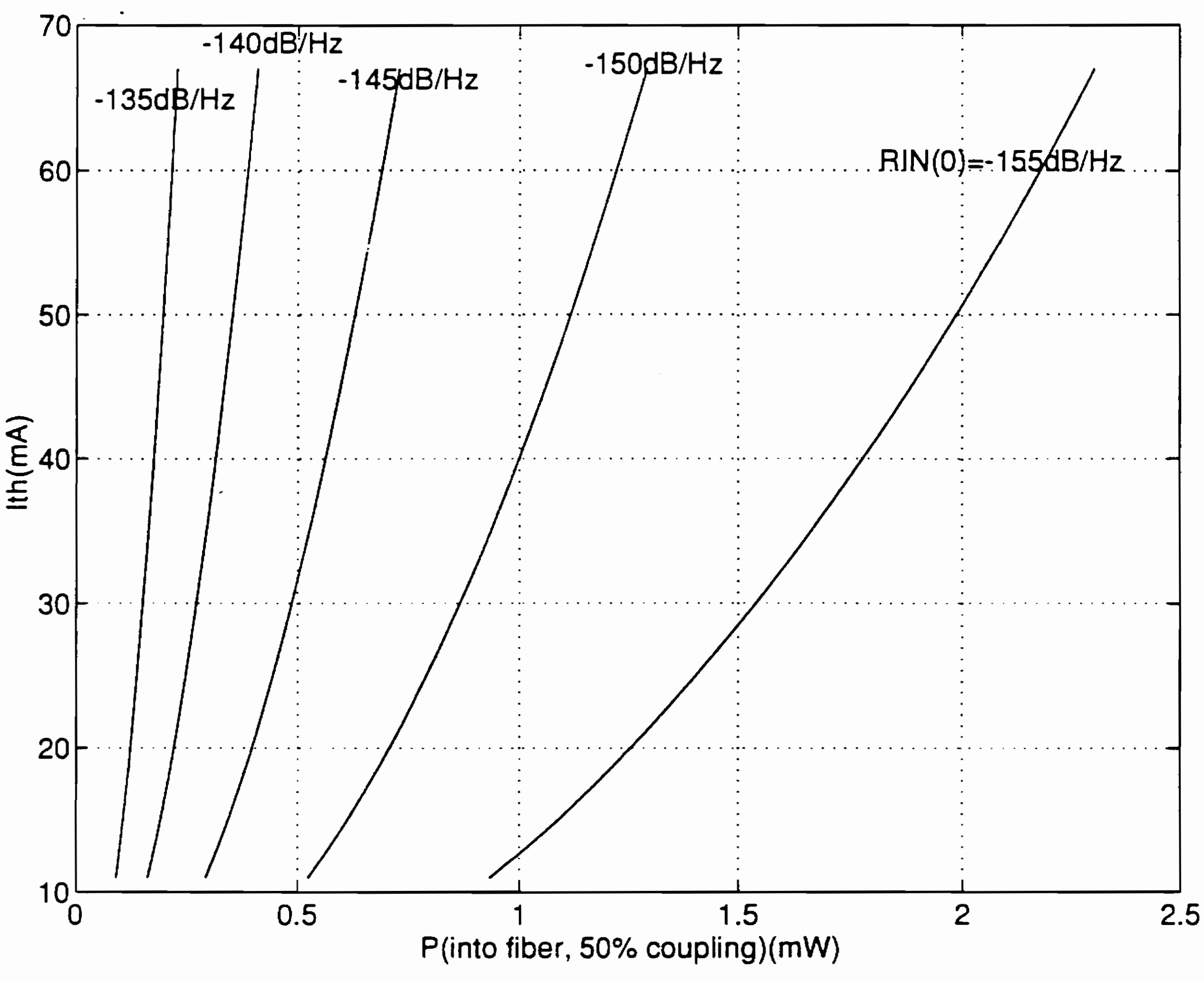

Figure 5.4 CONTOURS OF RIN(0) vs. POWER(I-Ith)&Ith

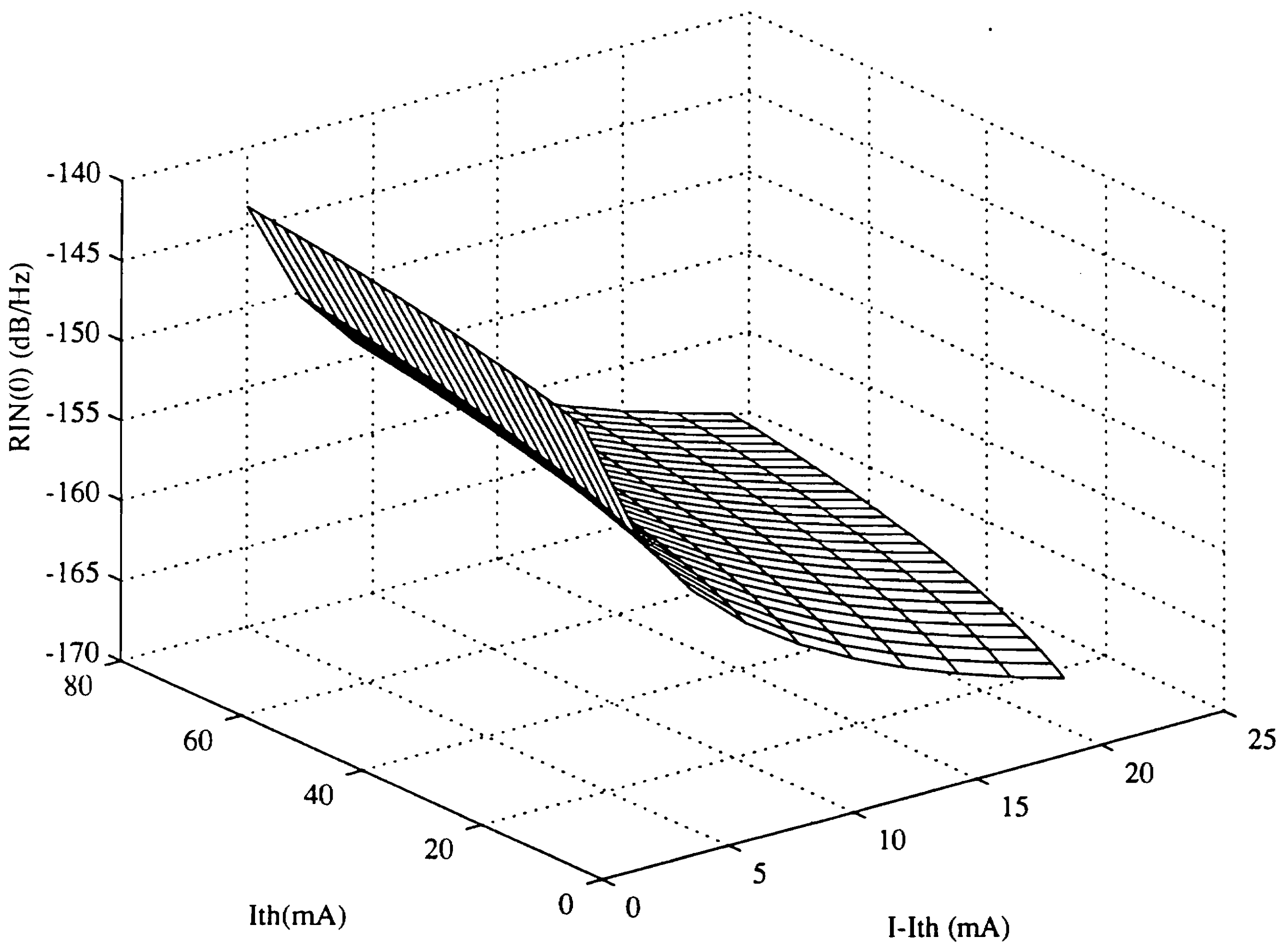

Figure 5.5 3-D PLOT OF RIN(0) vs. I-Ith&Ith

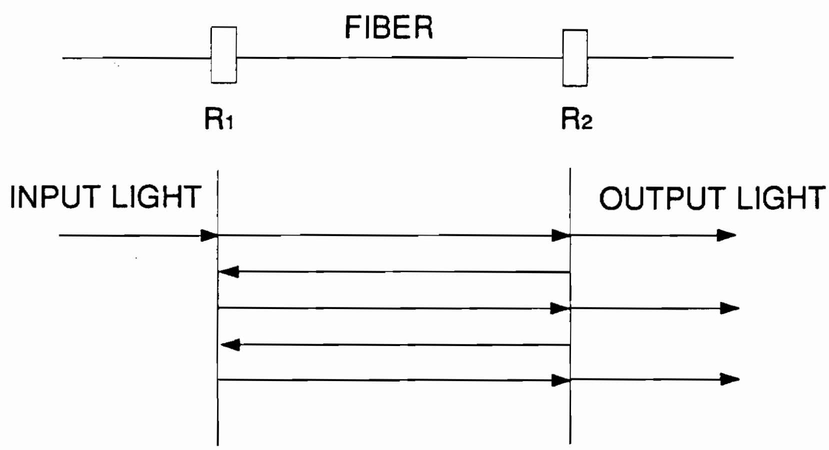

FIGURE 5.6 INTERFEROMETER FORMED BY TWO REFLECTION INTERFACES

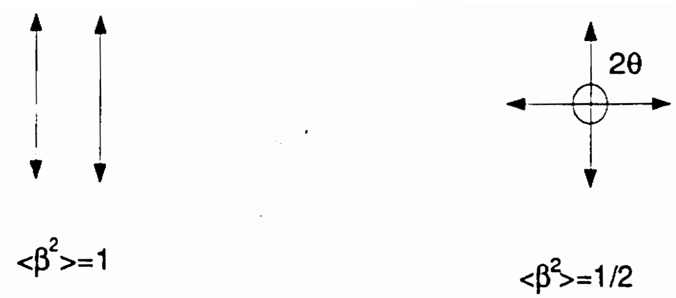

FIGURE 5.7 POLORIZATION FACTOR

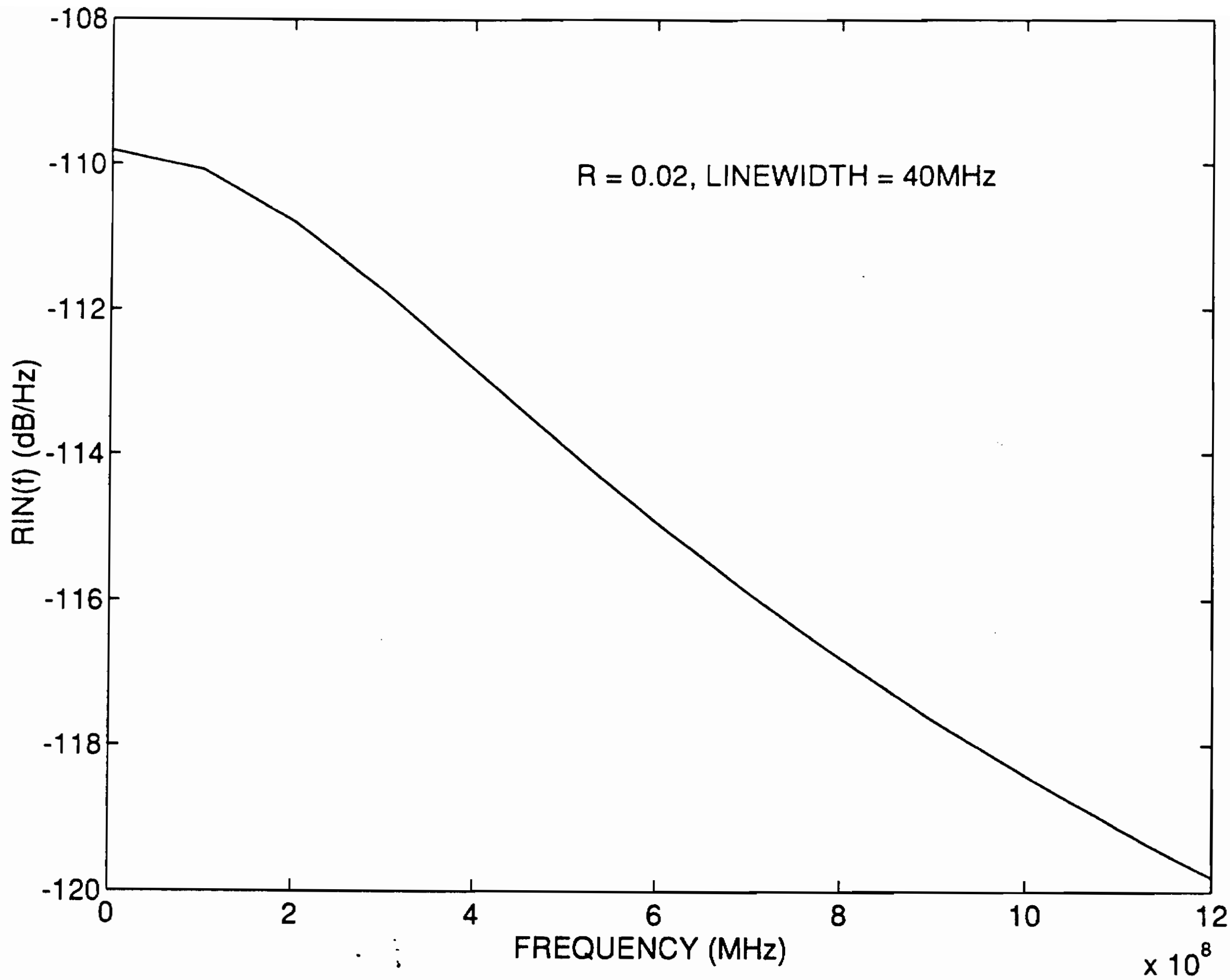

FIGURE 5.8 POWER SPECTRAL DENSITY OF RIN

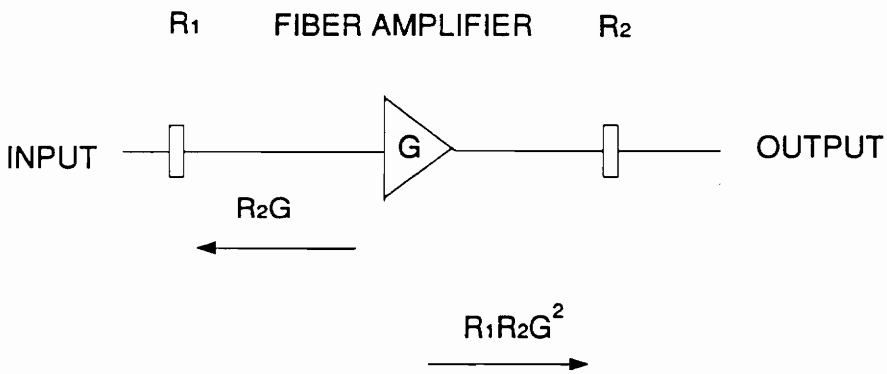

FIGURE 5.9 AMPLIFIED REFLECTION INDUCED NOISE

CHAPTER 6 NONLINEAR DISTORTION IN THE SYSTEM

As indicated in Part A, there is a separate requirement for the nonlinear distortion in a CATV distribution system. Three causes of nonlinear distortion, clipping distortion, chirp-dispersion distortion and gain tilt induced distortion, are described or analyzed in this section. It is shown that clipping distortion is the fundamental limit of our multichannel system and the other two are less important if lasers with small chirp are used.

6.1 Clipping Distortion

In a lightwave multichannel AM SCM system, the drive current modulating the laser diode can be expressed as

$$I(t) = I_b[1 + \sum_{j=1}^{N} m_j a_j \cos(2\pi f_j t + \phi_j)] \qquad (6.1)$$

where I_b is the bias current, m_j, a_j, f_j and ϕ_j are respectively the modulation index, the amplitude, the frequency, and the phase associated with the j-th RF subcarrier. The output light of the laser diode is generally proportional to the input current because of the linear nature of the light-current characteristic. Any deviation from the linearity distorts the optical waveform and may degrade the system performance. The rms optical modulation index μ, which is given by $\mu = m\sqrt{N/2}$ when a_j=1, increases with the number of channels N and the modulation index per channel m.

When the number of channels or the modulation index per channel exceeds a certain level, the total modulating current may fall below the laser threshold because of the near Gaussian distribution of the multichannel television signal. This results in the negative-peak-clipping of the intensity-modulated laser output, as shown in Fig 6.1. A. Saleh [5] first demonstrated that this nonlinearity of the laser diode is the fundamental limit of the channel capacity of optical multichannel AM SCM systems. However, he considered the clipping-induced nonlinear distortion as a noise term so that his result was overly conservative.

C. J. Chung and I. Jacobs [7][15] indicated that the clipping-induced nonlinear distortion should be considered separately from the noise and found that the rms modulation index must be less than 0.31 in order to meet the CSO and CTB requirement (-60dBc), as shown in Figure 6.2. As shown in Part A, the number of channels is proportional to the square of the rms modulation index if the other parameters are fixed. Therefore, the clipping distortion sets a fundamental limit on the channel capacity of the CATV distribution network.

6.2 Chirp-Dispersion Distortion

Amplitude modulation in semiconductor lasers is always accompanied by phase modulation because of carrier-induced changes in the modal index of refraction. Phase modulation can be included through the equation

$$\frac{d\phi}{dt} = \frac{1}{2}\beta_c\left(G_e - \frac{1}{\tau_p}\right) \qquad (6.2)$$

where β_c is the linewidth enhancement factor, ranging from 4 to 8, Ge is the net rate of stimulated emission and τ_p is the photon lifetime. By using small-signal analysis, the relation between the optical frequency excursion and the optical output intensity P(t) can be obtained as [14]:

$$\Delta\nu(t) = \frac{1}{2\pi}\frac{d\phi}{dt} = \frac{\beta_c}{4\pi}\kappa_\nu P(t) \qquad (6.3)$$

where βc is the linewidth enhancement factor and κ_v is a laser structure dependent constant. Then the phase term of the field $e^{-j\phi(t)}$ can be expressed as

$$\exp(-j\phi(t)) = \exp(-j\int \Delta v dt) = \exp(-j\frac{\beta_c}{4\pi}\kappa_v \int P(t)dt). \qquad (6.4)$$

The fiber dispersion can be expressed as a transfer function $H(\omega) = e^{-j\beta_2(\omega-\omega_0)^2 L/2}$. Thus, the output optical field from the fiber in frequency domain is given by

$$E_{out}(\omega) = E_{in}(\omega)H(\omega)$$
$$= \int \sqrt{P(t)}\exp(-j\frac{\beta_c}{4\pi}\kappa_v \int P(t)dt)\exp(-j\omega t)dt\, e^{-j\beta_2(\omega-\omega_0)^2 L/2} \qquad (6.5)$$

Since the input optical power is frequency dependent, as $P_{i}(t) = P_o[1 + \sum_{i}^{N} m_i(t)\cos(\omega_i t + \varphi_i)]$, the series expression of the above equation will include terms with different power dependencies and frequency dependencies. Therefore, the output optical power, which is $P = |E_{out}(\omega)|^2$, contains undesirable nonlinear distortion terms besides the signal [14] [25].

6.3 Coupling of Gain-Tilt and Chirp Induced Distortion

Since the gain spectrum of the EDFA is wavelength-dependent, the variation of the optical frequency caused by the laser chirp will result in a variation of the gain, which is called gain tilt. In single channel systems, the nonlinear distortion due to the gain tilt can be made negligible by operating the EDFA at the peak-gain wavelength. In our CATV distribution system, the EDFA is used to amplify the light with a few different wavelengths. Consequently, some of the signals may experience a certain amount of gain tilt. Therefore, it is necessary to investigate the nonlinear distortion caused by the coupling of gain-tilt and laser chirp.

The EDFA distortion results from FM to AM conversion in the amplifier. When the chirped modulated signal passes through the EDFA with wavelength dependent gain, $G(\nu)$, it experiences undesired amplitude modulation converted from frequency modulation and superimposed upon its desired amplitude modulation. The instantaneous optical input power (ignoring clipping) to the fiber amplifier can be written as [26] [27]:

$$P_i(t) = P_o[1+\sum_{i}^{N} m_i(t)\cos(\omega_i t+\varphi_i)] \qquad (6.6)$$

where P_o is the average optical power and $m_i(t)$ is the modulation index of channel i, ω_i, φ_i are the subcarrier frequency and the associated phase.

The gain of the EDFA may be expressed by

$$G(P,\lambda(t)+\lambda_o) = G_o + \frac{dG}{d\lambda}\Delta\lambda(t) \qquad (6.7)$$

Go is the gain at the center wavelength. $\Delta\lambda(t)$ depends on the optical power and the laser and may be written as [14]

$$\Delta\lambda(t) = \frac{\beta_c}{4\pi}\kappa P(t) = \frac{\beta_c}{4\pi}\kappa(P_o\sum_{i}^{N} m_i(t)\cos(\omega it+\varphi_i)) \qquad (6.8)$$

where κ is a laser structure dependent constant. With a characteristic fiber gain of $G(P, \lambda)$, the output power

$$P_o(t) = G(P,\lambda(t)+\lambda_o)P_i(t)$$

$$= G_oP_o[1+\sum_{i}^{N} m_i(t)\cos(\omega it+\varphi_i)] + P_o^2\frac{\beta_c}{4\pi}\kappa\frac{dG}{d\lambda}[\sum_{i}^{N} m_i(t)\cos(\omega it+\varphi_i) + (\sum_{i}^{N} m_i(t)\cos(\omega it+\varphi_i))^2] \qquad (6.9)$$

The square term contributes to the second order distortion. For the CSO at a specific channel band, we can calculate the number of components n falling within this band and then obtain

$$\mathrm{CSO} = 20\log\{P_o \frac{\beta_c}{4\pi} \kappa \frac{1}{G}\frac{dG}{d\lambda}[\sum_i^N m_i(t)\cos(\omega_i t+\varphi_i)]^2{}_n\}$$

where the subscript n means that only the appropriate n terms of the summation are taken. Using equation (6.8),

$$\begin{aligned}\mathrm{CSO} &\approx 20\log\{\frac{1}{G}\frac{dG}{d\lambda}\Delta\lambda m([\sum_i^N \cos(\omega_i t+\varphi_i)]^2{}_n)^{1/2}\}\\ &= 20\log\{\frac{1}{G}\frac{dG}{d\lambda}\Delta\lambda\mu\sqrt{\frac{2}{N}}\sqrt{n}\}\\ &= 20\log\{\frac{1}{G}\frac{dG}{d\lambda}\Delta\lambda\mu\sqrt{\frac{2n}{N}}\} \qquad (6.10)\end{aligned}$$

In the second step, we assumed that the modulation indexes are the same for different channels so that they can each be set equal to $\mu\sqrt{\frac{2}{N}}$. It is also assumed that the intermodulation terms add in phase. Equation (6.8) has been used and a factor of 1/2 comes from the average of cos function. For example, if the number of channels N=40, the rms modulation index μ is 0.3, the laser chirp $\Delta\lambda$=0.08nm, the gain G=12dB, $dG/d\lambda$=0.18dB/nm at the considered wavelength and the number of components n=12, then the CSO value calculated from equation (6.10) is -73.5dB. This satisfies the CATV requirement for CSO less then -60dBc.

6.4 Other Sources of Distortion

6.4.1 *Interchannel crosstalk*:

In multichannel systems, interchannel crosstalk may be an important impairment on the system performance. It is a fundamental limit on multichannel systems when semiconductor laser amplifiers (SLA's) are used. However, it is negligible when EDFAs are used. The interchannel crosstalk induced by carrier-density modulation does not occur when EDFAs are used for amplification of a multichannel signal, because EDFAs have a comparatively long recovery time τ (~10ms) and the practical channel spacing Ω exceeds 10MHz so that $\Omega\tau >> 1$. For densely packed WDM systems, the long gain recovery time is also an indication of the EDFA immunity to intermodulation distortion effects. Also, the crosstalk induced by cross-saturation can be avoided by operating the amplifier in the unsaturated region. Therefore, in the system we have been considering, we can neglect the distortion due to the interchannel crosstalk.

6.4.2 Stimulated Brillouin scattering:

When photons go through optical fibers, inelastic scattering, like Raman scattering and Brillouin scattering, occurs. The frequency of the scattered light is shifted downward during inelastic scattering. This is because the photon energy is reduced after scattering and the energy difference appears in the form of a phonon. Inelastic scattering results in a loss of the optical energy at the incident frequency and constitutes a loss mechanism for optical fibers.

When the optical power is very low, the loss due to inelastic scattering is negligible. However, at high power levels the nonlinear phenomena of stimulated Raman scattering (SRS) and stimulated Brillouin scattering (SBS) can make nontrivial contribution to fiber loss. The threshold power for both scattering can be estimated by considering how the scattered-light intensity grows from the noise. In the case of SBS the threshold power P_{th}, defined as the incident power at which half of the power is lost to SBS at the output end of a fiber of length L, is estimated from [28]

$$g_B P_{th} L_{eff} / A_{eff} \approx 21 \qquad (6.9)$$

where g_B is the Brillouin gain coefficient, L_{eff} is the effective interactive length which is defined as $L_{eff}=(1-\exp(-\alpha L))/\alpha$ and A_{eff} is the effective mode cross section, and α is the fiber attenuation per unit length. With $g_B \approx 5(10)^{-11}$ m/W for silica fibers, the value of P_{th} can be about 1mW near 1.55μm. But the bandwidth of large SBS is quite narrow so that the actual threshold power is increased to about 10mW. The threshold power of SRS is much larger than that of SBS because of its smaller gain coefficient. Figure 6.3 shows the CNR as a function of input power. It is seen that the CNR begins to decrease after the input optical power is larger than 8mW because of SBS. Therefore, an input optical power of 5mW is chosen in our CATV distribution system.

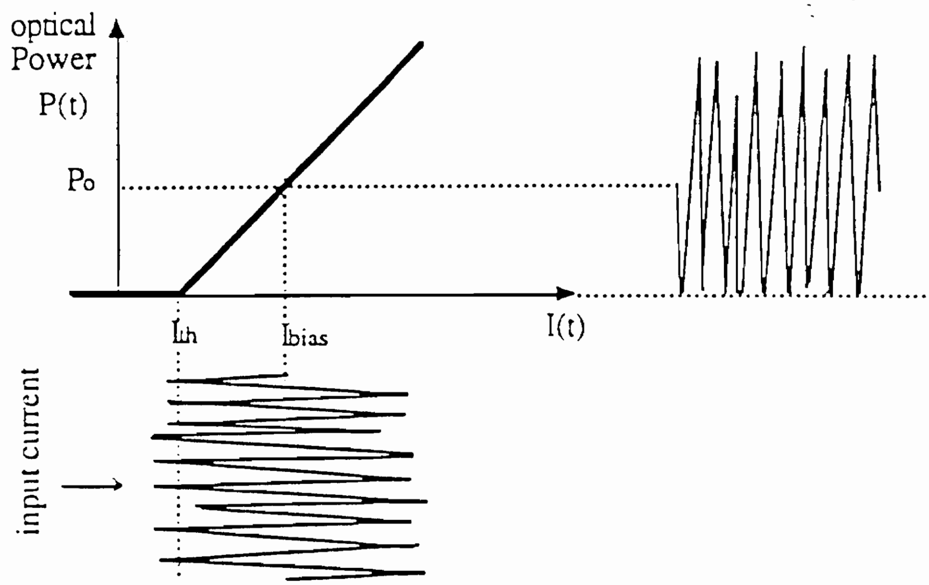

FIGURE 6.1 THE CLIPPING OF THE LASER OUTPUT
(TAKEN FROM REF[14])

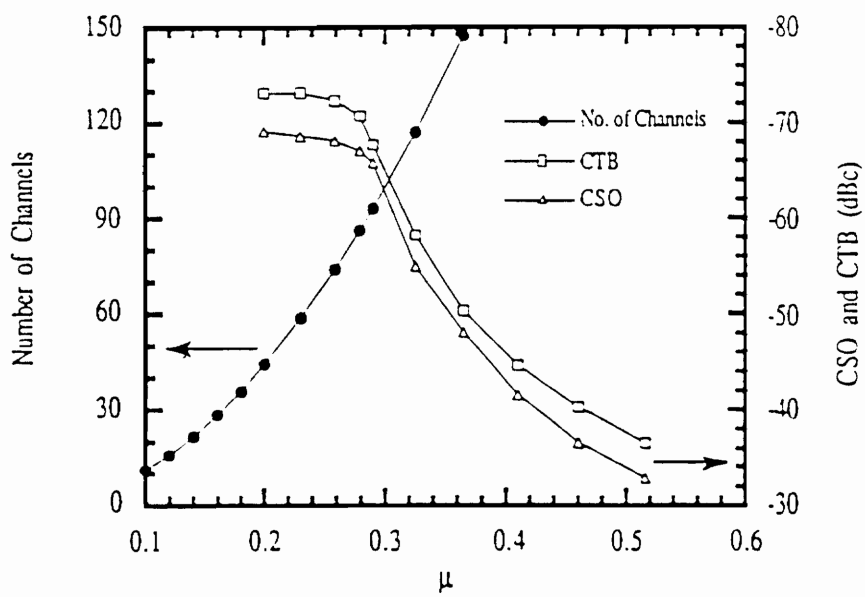

FIGURE 6.2 THE RELATION OF THE RMS MODULATION INDEX μ AND CSO, CTB. (TAKEN FROM [7])

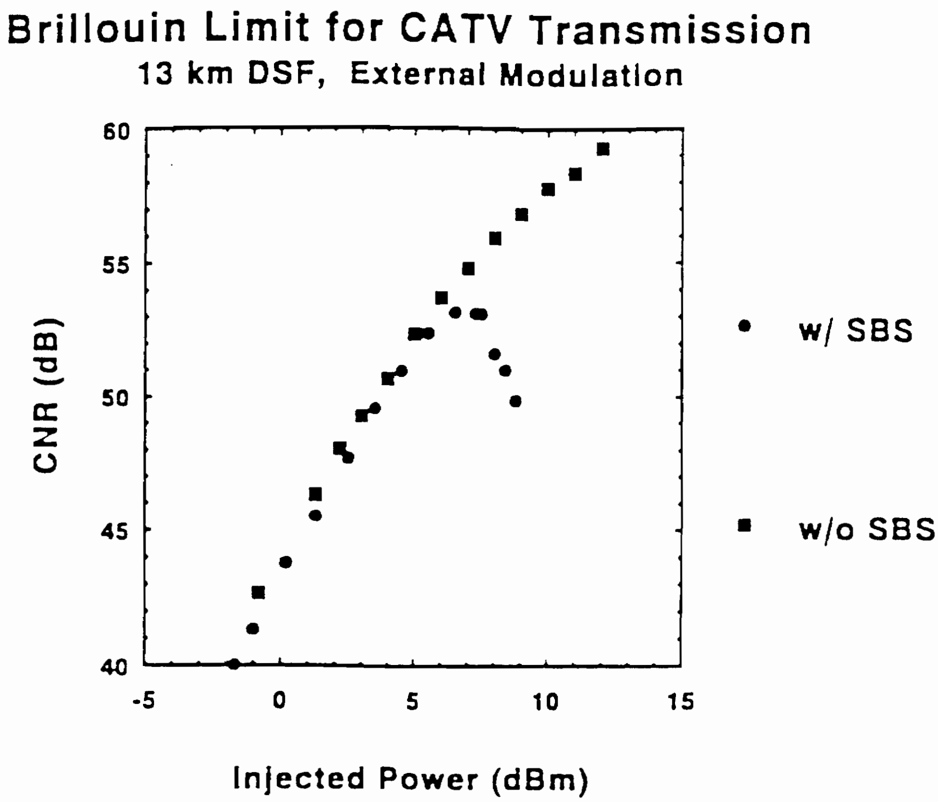

FIGURE 6.3 CNR AS A FUNCTION OF INPUT OPTICAL POWER FOR SBS. (TAKEN FROM [29])

CHAPTER 7 OPTICAL AMPLIFIER MODELING

The modeling is based on the two-level model starting from the modified rate equations. The lengths of the EDFAs are chosen to optimize the system performance. In this thesis they are approximated by the lengths to achieve the maximum gains given the values of the signal powers and the pump powers into the EDFAs after the first-stage star coupler. The gains and the spontaneous-emission factors are obtained after the lengths are chosen.

7.1 Modeling of Gain of the EDFA:

The two-level model is used to calculate the gain and the spontaneous emission factor of EDFAs pumped at the wavelength of 1480nm. Although the 980nm-pumped EDFA involves three level energy states, [11] shows that for typical fiber amplifier parameters, treating the 980-nm pumped amplifier with a two-level model is valid for average pump powers less than 1 W. This condition is satisfied in the case of two-stage couplers since the pump power is split by the star coupler. This implies that the population in the $^4I_{11/2}$ state is negligible. Also, the pump excited-state absorption is assumed not to occur here. If $N_2(r,\varphi,z,t)$ is the fractional population of the upper state, normalized by the total erbium ion density $N_t(r,\varphi,z,t)$, and $N_1(r,\varphi,z,t)$ is the fractional population of the lower state, we have

$$N_1(r,\varphi,z,t)+N_2(r,\varphi,z,t)=1 \quad . \qquad (7.1)$$

The light propagating in the amplifier is modeled as a number of optical beams with optical wavelengths λ_k. If the light intensity distribution in cylindrical coordinates is $I_k(r,\varphi,z,t)$, the optical power of the kth beam is [30]

$$P_k(z,t) = \int_0^{2\pi}\int_0^{a} I_k(r,\varphi,z,t) r dr d\varphi \tag{7.2}$$

and the normalized optical intensity is defined as

$$i_k(r,\varphi,t) = I_k(r,\varphi,z,t) / P_k(z,t) \tag{7.3}$$

where a is the core radius of the erbium-doped fiber.

For the two-level amplifier model, the rate equation for the population of the upper state is

$$\frac{\partial N_2(r,\varphi,z,t)}{\partial t} = -\frac{N_2(r,\varphi,z,t)}{\tau_{sp}} - \sum_k P_{in}^k i_k \sigma_{ak} N_1(r,\varphi,z,t) - \sum_k P_{in}^k i_k \sigma_{ek} N_2(r,\varphi,z,t) \tag{7.4}$$

where P_{in}^k is the input optical power normalized by photon energy hv, or the input photon number at wavelength λ_k.

$$\frac{\partial P_{in}^k(r,\varphi,z,t)}{\partial z} = u_k\sigma_{ek}\int_0^{2\pi}\int_0^{a} i_k(r,\varphi) N_2(r,\varphi,z,t)(P_{in}^k(r,\varphi,z,t) + m\Delta v_k) r dr d\varphi$$
$$-u_k\sigma_{ak}\int_0^{2\pi}\int_0^{a} i_k(r,\varphi) N_1(r,\varphi,z,t) P_{in}^k(r,\varphi,z,t) r dr d\varphi \tag{7.5}$$

where $m\Delta v_k$ is the contribution of spontaneous emission, u_k refers to the traveling direction either 1 (forward) or -1 (backward). σ_{ek} and σ_{ak} are the cross sections for stimulated emission and absorption at wavelength λ_k. Since the input signal power is relatively large, the contribution of spontaneous emission is negligible and m is considered to be zero in the subsequent derivation.

Under steady-state conditions, the populations and optical powers are independent of time. $N_2(r,\varphi,z,t)$ can be obtained by setting the left side of equation (7.4) equal to zero. For simplicity, we do not need to consider the spatial dependence but use the average figures. Then equation (7.5) can be written as

$$\frac{dP_{in}^k(z)}{P_{in}^k(z)} = -u_k N_t \sigma_{ak} \Gamma_k dz - \sum_{i}^{N} u_k \sigma_{ek} dP_{in}^k(z,) \tag{7.6}$$

where we have used

$$\frac{dP_{in}^k(z)}{dz} = u_k N_t \Gamma_k (\sigma_{ek} N_2 - \sigma_{ak} N_1) P_{in}^k(z,) \qquad (7.7)$$

and σ_{ek} is zero when the kth beam is the pump beam. Integrating the equation, we get

$$P_{out}^k = P_{in}^k e^{-\alpha_k L} e^{\sum_j^N (P_{in}^j - P_{out}^j)/P_{sat}^k} \qquad (7.8)$$

where P_{in}^k and P_{out}^k are the input (z=0) and output (z=L) powers at wavelength λ_k. P_{sat}^k is the intrinsic saturation power at wavelength λ_k. Then the total output power at z=L is [11]

$$P_{out} = \sum_{k=1}^{N} C_k e^{-P_{out}/P_{sat}^k}, \text{ where } C_k = P_{in}^k e^{-\alpha_k L} e^{P_{in}/P_{sat}^k}. \qquad (7.9)$$

If the absorption constant α_k, the intrinsic saturation powers and the input powers for each wavelength are known, the total output power can be solved from this equation.

Given the input signal power and the pump power, the gain of the EDFA can be calculated from the above equations. Figure 7.1 shows the results. With a signal power of 0dBm and a pump power of 20dBm, a gain of 17dB is obtained. It follows from the plot that the threshold pump power is a constant regardless of the input power.

7.2 Spontaneous Emission Factor:

The spontaneous-emission factor n_{sp} depends on the relative populations N_1 and N_2 of the ground and excited states as $n_{sp} = \frac{N_2}{N_2 - N_1}$. From the above analysis, it is known that N_1 and N_2 vary along the erbium-doped fiber length due to their dependence on the pump and signal powers. Therefore the noise figure is expected to depend both on the amplifier length L and the pump power P_p, just as the amplifier gain does. Ignoring the absorption of spontaneous emission power, the average spontaneous-emission factor can be calculated with the following formula obtained from the rate equation (7.4)

$$n_{sp} = \frac{\int_0^L g(v) n_2(z) G(L-z) dz}{G-1} \qquad (7.10)$$

The calculated n_{sp} as a function of the input signal power and pump power is shown in Figure 7.2. When the pump power becomes large (>20dBm) and the signal power is very small (<-5dBm), the spontaneous emission factor is close to 1. The larger the pump power is, the smaller is n_{sp}.

In our modeling, the length of the EDFA is chosen to achieve the maximum gain with the given pump power [31]. This length may be slightly different from the actual optimal EDFA length which achieves the best system performance. The resulting difference should not be very significant. Figure 7.3 shows the EDFA length as a function of the input signal power and pump power. It is seen that the length is nearly proportional to the pump power and decreases slightly with increasing signal power.

Parameters used in the system modeling are: the optical power P at the input to the first star coupler is 5mW, the single pump power Pp is 200mW, the bandwidth B_e (chosen to be the effective noise bandwidth) is 4MHz for video signals, the fiber length between the transmitters and receivers is 10km, and the value of CNR is fixed at 50dB. G and n_{sp} are then obtained from the modeling outlined above, and the number of channels is calculated from the complete equation (3.2) given a pair of M and K.

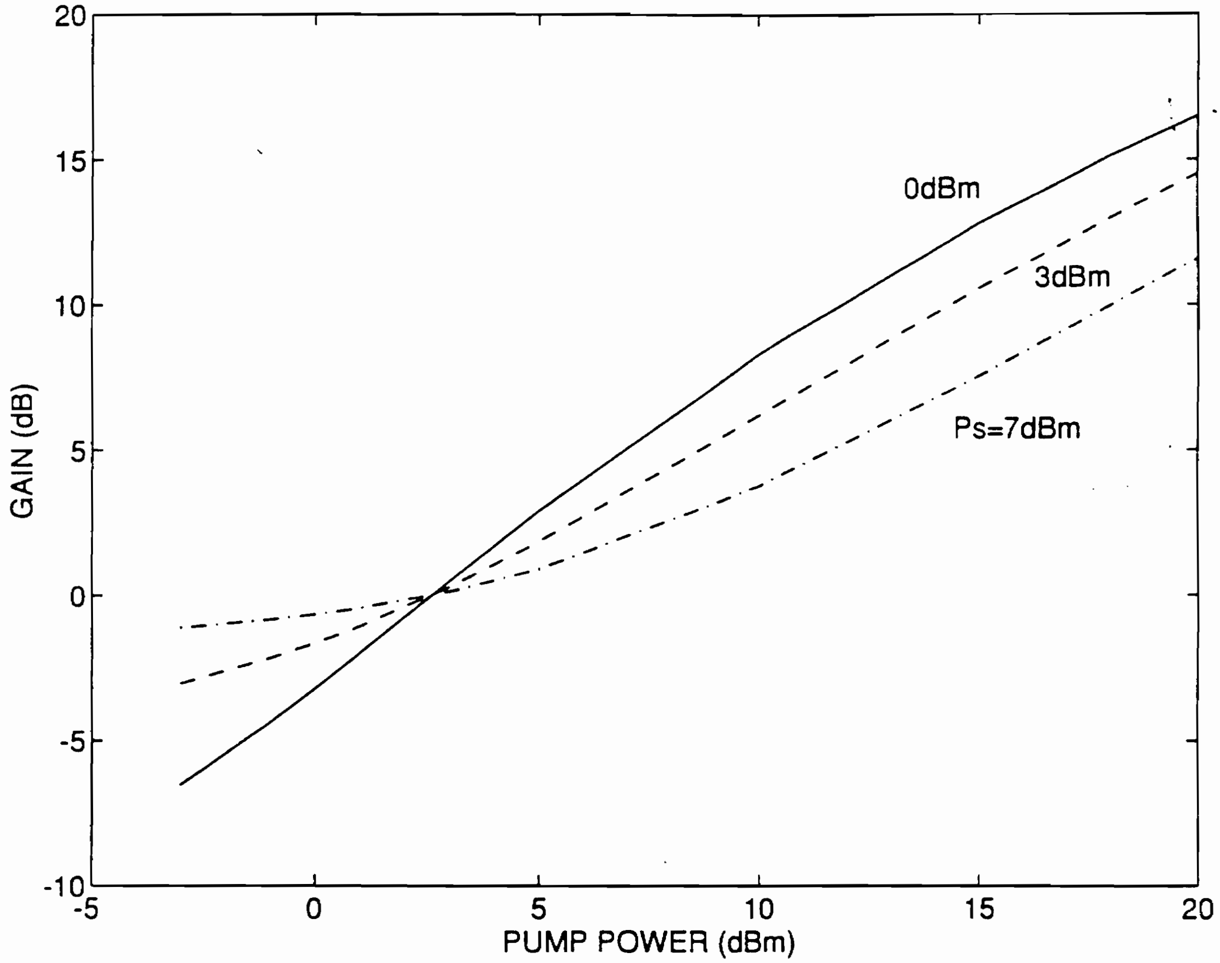

FIGURE 7.1 GAIN AS A FUNCTION OF PUMP POWER AT 1480nm

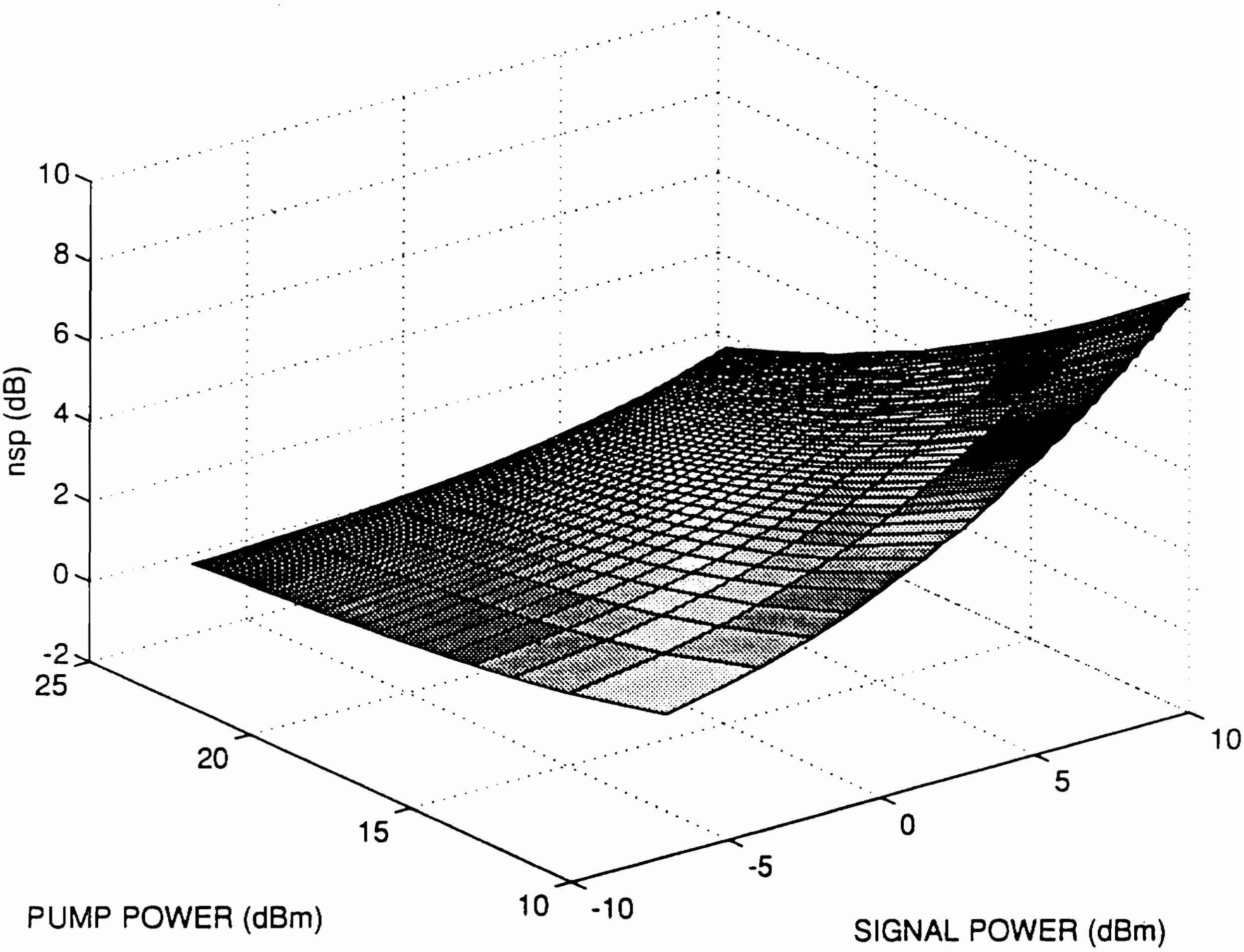

FIG. 7.2 SPONTANEOUS-EMISSION FACTOR AS A FUNCTION OF Ps & Pp

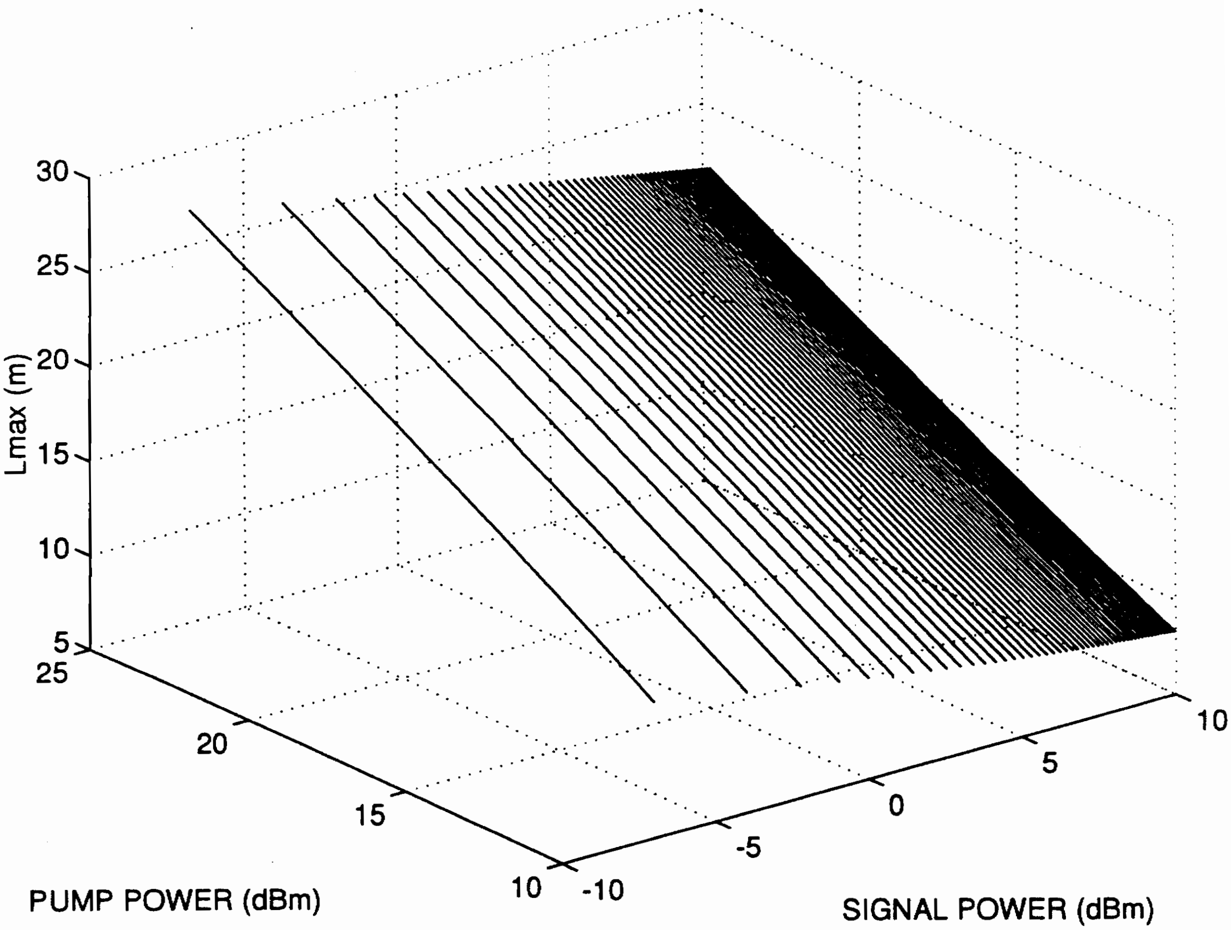

FIG 7.3 OPTIMAL EDFA LENGTH AS A FUNCTION OF Ps & Pp

CHAPTER 8 SUMMARY AND SUGGESTIONS

8.1 Summary

In this thesis, the effects of noise in AM-VSB SCM CATV distribution networks is evaluated for different configurations. In the systems with optical amplifiers and star couplers, the performance and capacity are determined not only by the received optical power but also by the performance of the optical amplifiers. An optimum length of the EDFA may be chosen to achieve the best system performance.

Based on the results of computer modeling, it is found that a double-star network with individually pumped optical amplifiers between the two stars provides a better system performance and capacity than either a baseline single star network, or a double star network in which the amplifiers share a common pump fed through the first star coupler. The number of output nodes may be increased to 322 or 572 by using a 2X2 first-stage star coupler followed by two EDFAs or a 4X4 first-stage star couplers followed by four EDFAs, compared to 160 nodes for the baseline network. The total number of channels which may be distributed is increased from the 80-channel limit of a single link to more than 300 channels by using optical amplifiers and the WDM technique.

Since the results are dependent on assumptions concerning the noise, the critical sources of noise are identified and modeled. As proved in Section 5.2, quadruply reflected field makes a negligible difference on the power spectral density of Reflection Induced Noise. However, it is shown in Section 5.4 that Reflection Induced Noise can be enhanced by optical amplifiers, and the reflection enhances amplified spontaneous noise. Hence, the reflections in the networks need to be kept small. Also in

Chapter 5, the power behavior of laser intrinsic RIN is analyzed. It is shown that in the case of large signal, RIN(0) becomes proportional to the inverse square of output optical power.

A formula to calculate the value of composite-second-order distortion (CSO) due to coupling of gain-tilt and chirp is obtained in Section 6.3. In the systems we are considering, this distortion is not severe. Clipping distortion due to the nonlinearity of the laser is the main limitation on the system capacity.

The gain and spontaneous emission factor of the EDFA is obtained by modeling based on the laser rate equation. The performance of EDFA depends closely on the pump power as well as the pumping method. The length of EDFA may be optimized to improve the performance given the pump power and input signal power.

8.2 Suggestions for Future Studies

In order to get more practical results, more precise modeling needs to be done. Many combined effects should be taken into account, and a broader range of optical parameters should be considered. Also, the effects of modulation on the electrical spectrum of the signals needs to be specified and analyzed. To make clipping distortion smaller than the required value, we assume that the maximum RMS modulation index should not exceed 0.3. This is based on measurements and simulations for 40 channel systems. This may vary when the number of channels is many more than 40. Experiment or simulation is needed to see the difference.

The discrepancy of the large-signal behavior of laser RIN between the result in this thesis and that quoted in the literature needs to be tested by experiment. There might be some unknown factors affecting the result. It was shown in Section 5.2 that the higher order of reflections does not significantly affect reflection induced noise. However, experiments generally show that the actual value is larger than the analytic result. The difference may be contributed by multiple reflections between multiple reflectors, and some other effects.

When the WDM technique is employed, many other effects may degrade the system performance. In addition to the intermodulation in the electrical domain, the optical interference may occur between the channels which are modulated at the same subcarrier frequency but transmitted at different wavelengths. This should be investigated. Techniques to reduce the gain tilt, including appropriate selection of the optical wavelengths, should also be investigated.

Coupling of gain-tilt and chirp is also an issue worth further investigation. Since its physical principle is quite similar to the chirp-dispersion, there might be an equalization way to reduce the resulting distortion.

It may be useful for fiber CATV industries to get an empirical expression of the relation of the spontaneous emission factor, the signal power and the pump power as well as the parameters of EDFA, so that detailed modeling of EDFAs is not required for system evaluation.

APPENDIX

THE EFFECT OF RIN IN DIGITAL SYSTEMS

In Part A, the effect of RIN in analog systems is considered. Since the optical power in digital systems is generally much smaller than in analog systems, RIN in digital systems has much less impact on the system performance than in analog systems. However, in high-speed digital systems, the laser is not completely turned off in the off state. The ratio of the photocurrent in the off state and the on state, which is called the extinction ratio, is therefore not equal to zero. The combined effect of RIN and non-zero extinction ratio may become significant. In addition, optical amplifiers used in the systems enhance these effects.

I. *THE POWER PENALTY RESULTING FROM COMBINED EFFECT OF RIN AND NON-ZERO EXTINCTION RATIO:*

When the extinction ratio is non-zero, there is shot noise and RIN in addition to thermal noise in both the on and off states.

$$\begin{aligned}
\mu_1 &= Ip \ , \\
\mu_0 &= \varepsilon \, Ip \, , \\
\sigma_1{}^2 &= 2\,q\,Ip\,B_e + 4\,k\,T\,B_e/R_e + \alpha^2\, I_p{}^2 B_e \, , \qquad \text{(A-1)} \\
\sigma_0{}^2 &= 2\,q\,\varepsilon Ip\,B_e + 4\,k\,T\,B_e/R_e + \alpha^2\,\varepsilon^2 I_p{}^2 B_e \, ,
\end{aligned}$$

where μ_1 and σ_1 are the mean and standard deviation of the signal at the output of the receiver when a 1 is transmitted; μ_0 and σ_0 are the mean and standard deviation of the signal at the output of the receiver when a 0 is transmitted. α^2 is the RIN factor and ε is the extinction ratio. R_e is the effective noise resistance of the receiver. Defining the effective capacitance $C_e = \frac{1}{2\pi B_e R_e}$, we obtain the sensitivity in photons-per-bit (N_p)

$$N_p = \frac{Q^2 B_e}{\eta B}\frac{1+\varepsilon}{1-\varepsilon}\frac{1+\frac{1}{Q}\sqrt{\frac{8\pi C_e V_T}{q}}}{1-Q^2\frac{1+\varepsilon}{1-\varepsilon}\alpha^2 B_e-\frac{2Q\varepsilon}{1-\varepsilon}\frac{1}{\sqrt{\frac{8\pi C_e V_T}{q}}}} \tag{A-2}$$

where Q=6 for a 10^{-9} error probability. Then the power penalty due to the non-zero extinction ratio with the RIN taken into account is

$$\text{Power penalty} = -10\log\left(\frac{1+\varepsilon}{1-\varepsilon}\left[1-Q^2\frac{1+\varepsilon}{1-\varepsilon}\alpha^2 B_e-\frac{2Q\varepsilon}{1-\varepsilon}\frac{1}{\sqrt{\frac{8\pi C_e V_T}{q}}}\right]\right) \tag{A-3}$$

where, the last term is generally more significant than the second term in the parenthesis. There is an error floor at

$$Q_{max} = \frac{\left[(\varepsilon/a)^2+4\alpha^2 B_e\right]^{1/2}-\frac{\varepsilon}{a}}{2(1+\varepsilon)\alpha^2 B_e} \tag{A-4}$$

where, $a = \sqrt{\frac{8\pi C_e V_T}{q}}$.

Note that the above derivation assumes that the receiver thermal noise is large compared to the shot noise.

Figure A.1 shows power penalty as a function of the extinction ratio for different values of α^2 as calculated from equation (A-3). We assume the transmission bit rate B and the receiver bandwidth B_e are 1GHz and 0.7GHz respectively. RIN of the order -120dB gives a 0.2dB increase of power penalty compared with RIN-absent result. RIN of the order -110dB/Hz leads to 2dB power penalty when the extinction ratio is small, and up to 5dB when the extinction ratio is 0.2. Fortunately, RIN is normally less than -135dB/Hz. Figure A.2 shows that only when RIN is greater than -120dB/Hz will it have a significant effect. Note that if RIN exceeds -105dB, the power penalty becomes infinite even at zero extinction ratio.

II. PERFORMANCE OF RECEIVER WITH AN OPTICAL PREAMPLIFIER:

In order to improve the system performance, an optical amplifier is often used before the receiver to compensate for the power loss in the fiber. However, the amplifier introduces some additional noise, of which the main contributions are the signal-spontaneous beat noise and the spontaneous-spontaneous beat noise. In this section, the receiver sensitivities with an optical amplifier in the cases of RIN-present and non-zero extinction ratio are discussed.

a. The effect of RIN on the performance:

In the absence of modulation, the electric field incident on the photodetector can be written as

$$E = [A + a(t) + x(t)]\cos(\omega_c t + \theta(t)) + y(t)\sin(\omega_c t + \theta(t))$$

where A is the amplitude of the field, a(t) is the amplitude fluctuation due to RIN, θ(t) is the phase noise, and x(t) and y(t) are the in-phase and quadrature components (relative to the signal phase) of the amplified spontaneous emission (ASE) noise.

The output of the detector is then given by [12]

$$I = \frac{1}{2}A^2 + Aa + Ax + 2x^2 = I_s + I_{RIN} + I_{s-sp} + I_{sp-sp} \qquad \text{(A-5)}$$

where we have ignored the shot noise and thermal noise assuming G is sufficiently large. The total electrical noise is given as the sum of the variances of the individual noise currents. Their variances have been derived in [4] as

$$\mathrm{var}\, I_{RIN} = (RIN) I_s^2 B_e$$

$$\mathrm{var}\, I_{s-sp} = 2 I_s I_{ASE} B_e / B_o$$

$$\mathrm{var}\, I_{sp-sp} = I_{ASE}^2 B_e / B_o$$

$$\mathrm{var}\, I_{RIN-sp} = \frac{1}{4}(RIN) I_s I_{ASE} B_e$$

and $I_{ASE} = R 2 n_{sp} h\nu (G-1) B_o$, G is the gain of the amplifier and R is the effective responsivity.

Assume all the noises are Gaussian distributed, then for an OOK system,

$\mu_1 = Ip + I_{ASE}$,

$\mu_0 = I_{ASE}$,

$\sigma_1{}^2 = 2\, q\, (Ip + I_{ASE}) B_e + 4\, k\, T\, B_e/R_e + \alpha^2\, I_p{}^2 B_e + I_{ASE}{}^2 B_e/B_o + 1/4\, Ip I_{ASE} \alpha^2 B_e$

$\sigma_0{}^2 = 2\, q\, I_{ASE}\, B_e + 4\, k\, T\, B_e/R_e + I_{ASE}{}^2 B_e/B_o$, where the shot noise and thermal noise are included but will be ignored in the subsequent derivation. Then we obtain the receiver sensitivity

$$N_p = \frac{2n_{sp}QB_e}{R_b}\frac{G-1}{G}\frac{1}{1-Q^2\alpha^2 B_e}[1+\frac{1}{8}\alpha^2 B_o+\frac{1}{Q}\sqrt{\frac{B_o}{B_e}}] \tag{A-6}$$

Normally, the value of α^2 is the order of less than -140dB/Hz and $\alpha^2 B_e<10^{-3}$ so that RIN does not affect the system performance significantly even if the optical amplifier is employed before the receiver. It should be noted that there is a term containing the product of RIN and optical bandwidth, which implies that if the bandwidth of the optical filter is relatively large, RIN could affect the performance significantly.

b. The effect of non-zero extinction ratio:

$\mu_1 = Ip+I_{ASE}$,

$\mu_0= \varepsilon\, Ip+I_{ASE}$,

$\sigma_1{}^2 = 2q\,(Ip+I_{ASE})B_e+4kTB_e/R_e+I_{ASE}{}^2B_e/B_o+2IpI_{ASE}B_e/B_o$

$\sigma_0{}^2 = 2\,q\,(\varepsilon Ip+I_{ASE})B_e + 4\,k\,T\,B_e/R_e + I_{ASE}{}^2B_e/B_o +2\varepsilon IpI_{ASE}B_e/B_o$,

Similar to (a), we neglect the shot noise and thermal noise and get the following expression

$$N_p = \frac{2n_{sp}Q^2B_e}{R_b}\frac{G-1}{G}(\frac{1+\varepsilon}{1-\varepsilon})^2\left\{1+[1-(\frac{1-\varepsilon}{1+\varepsilon})^2(1-\frac{B_o}{Q^2B_e})]^{1/2}\right\} \tag{A-7}$$

If we let α^2 and ε equal zero, then both the equations (16) and (17) lead to the same expression for the receiver sensitivity with the optical preamplifier. But the extinction ratio plays a much stronger role degrading the performance. The power penalty increases more than a factor of $\frac{1+\varepsilon}{1-\varepsilon}$ compared with the case of optical-amplifier-absent. Figure A.3 is the plot of power penalty versus the extinction ratio with different values of the optical filter bandwidth. It is seen that the larger the optical bandwidth, the smaller is the power penalty from the non-zero extinction ratio. However, the absolute receiver sensitivity degrades as the optical bandwidth increases. This is shown in Figure A.4, in which receiver sensitivity is plotted as a function of the optical bandwidth for $\varepsilon = 0$, 0.1 0.2.

c. The combined effect of RIN and non-zero extinction ratio:

Taking into account both RIN and non-zero extinction ratio, we get an expression for the sensitivity

$$N_p = \frac{2 n_{sp} Q^2 B_e}{R_b} \frac{G-1}{G} \left(\frac{1+\varepsilon}{1-\varepsilon}\right)^2 \frac{1}{\left(1-\frac{1+\varepsilon}{1-\varepsilon}\Omega\right)^2} \bullet$$
$$\left\{(1-\Omega)(1+\beta)+\left[(1-\Omega)^2(1+\beta)^2-\left(\frac{1-\varepsilon}{1+\varepsilon}\right)^2\left(1+\beta-\frac{B_o}{Q^2 B_e}\right)\right]^{1/2}\right\} \tag{A-8}$$

where $\Omega = Q^2\alpha^2 B_e$, $\beta = \frac{1}{8}\alpha^2 B_o$. Power penalty as a function of extinction ratio is plotted in Figure A.5 for various values of RIN. It is seen that the effect of RIN is non-trivial if the order of RIN is greater than -120dB/Hz.

For the case of non-zero extinction ratio, the RIN in off state is 20dB/Hz larger than in on state, which is shown in Figure A.6.

III. DISCUSSION:

Normally, RIN is so small that the effect is negligible in digital systems. However, the power penalty resulting from the combined effect of RIN and non-zero extinction ratio could be significant when either one is large enough. An error floor exists and sets a maximum limit on allowable RIN. The use of an optical preamplifier does not change the effect of RIN but makes the deterioration due to the non-zero extinction ratio much more severe.

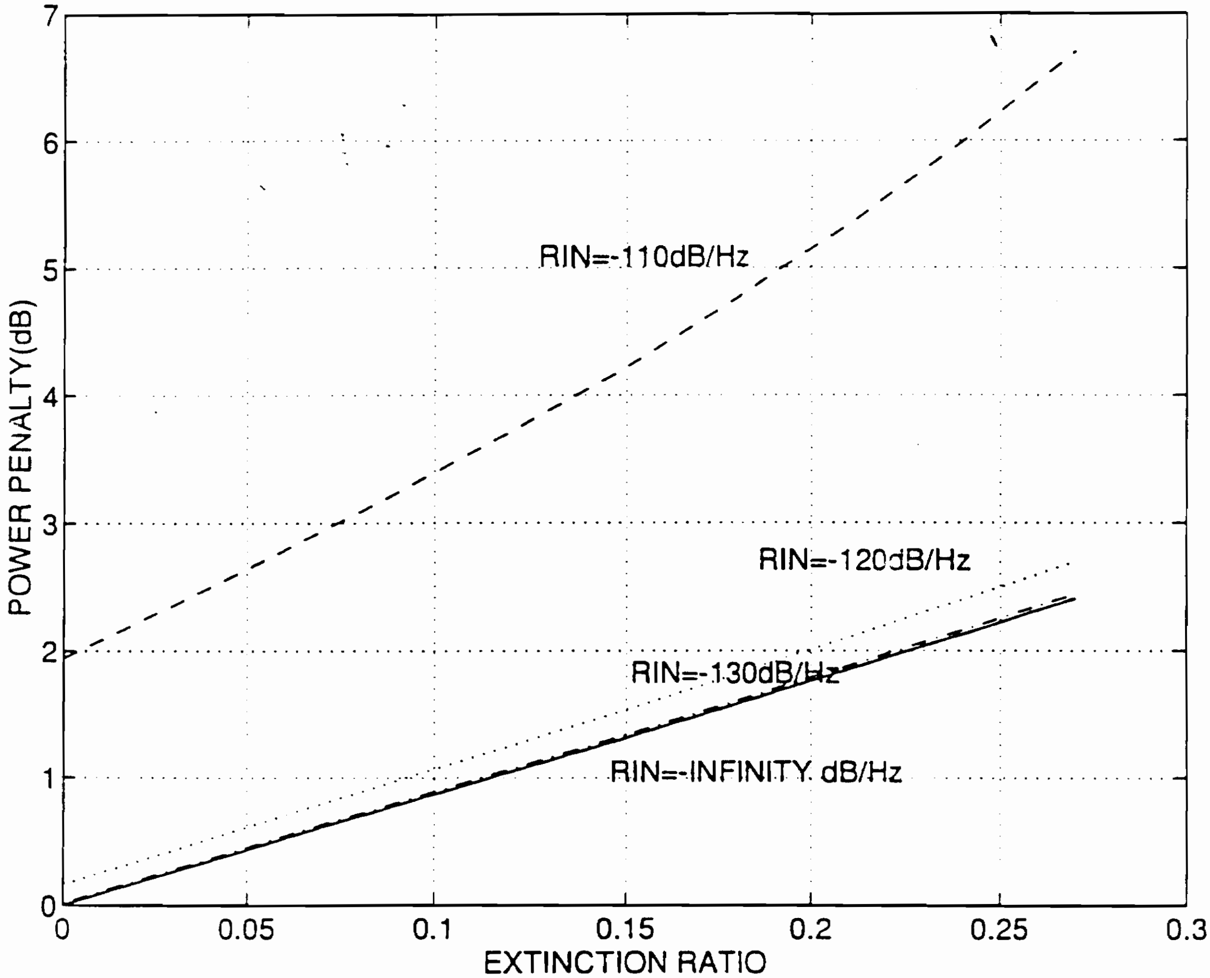

FIGURE A.1 POWER PENALTY DUE TO RIN&NON-ZERO EXTINCTION RATIO

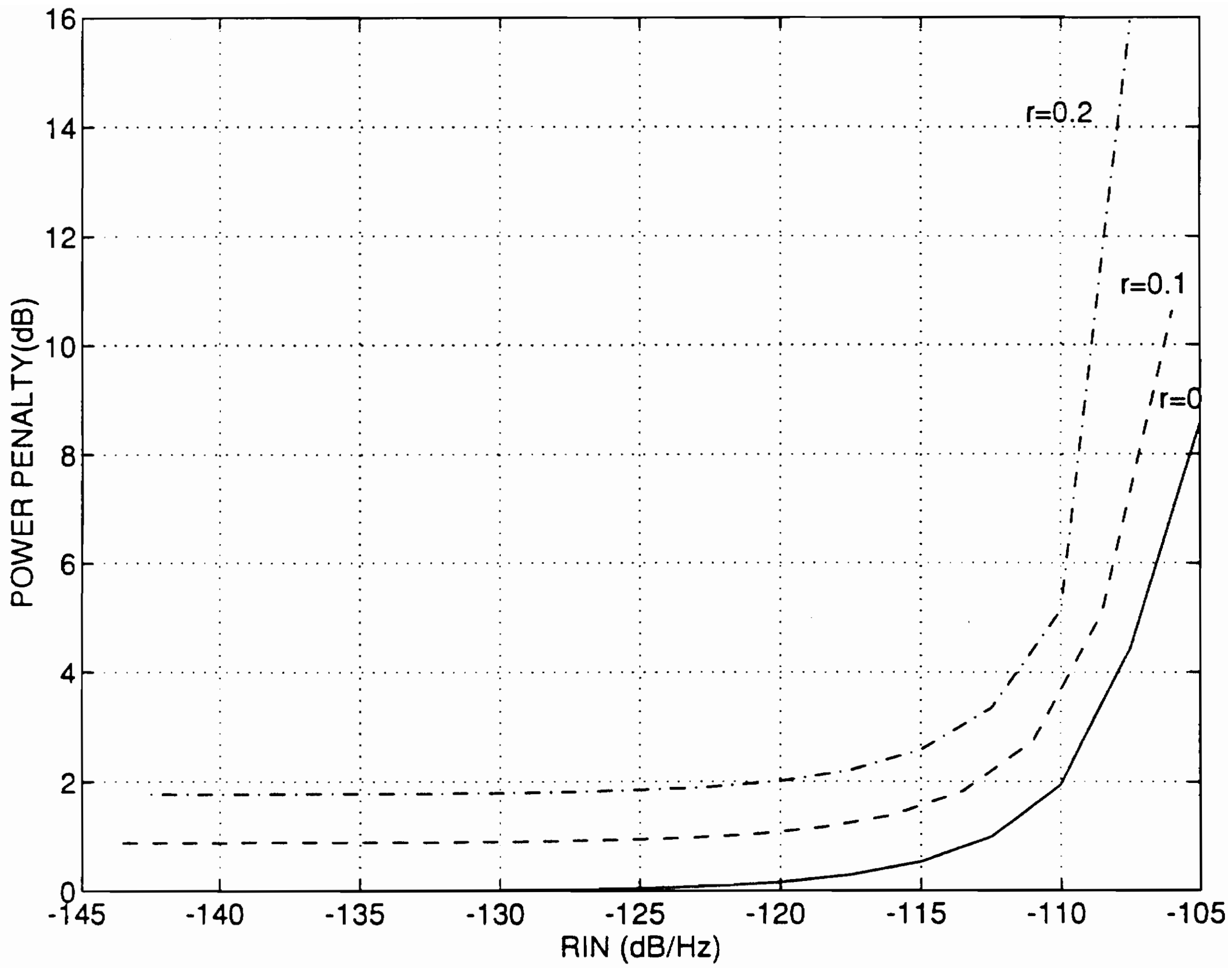

FIGURE A.2 POWER PENALTY DUE TO RIN&NON-ZERO EXTINCTION RATIO

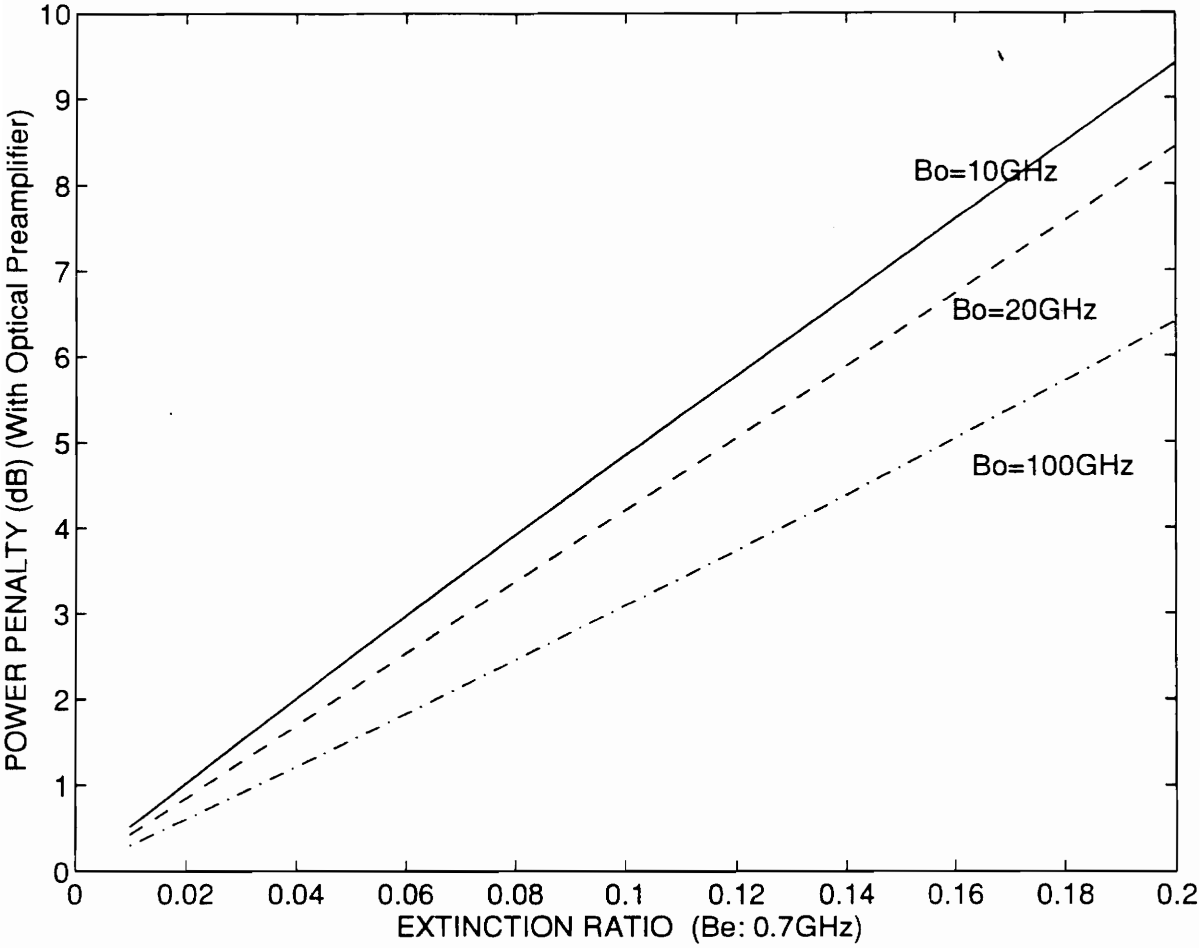

FIGURE A.3 POWER PENALTY DUE TO NON-ZERO EXTINCTION RATIO

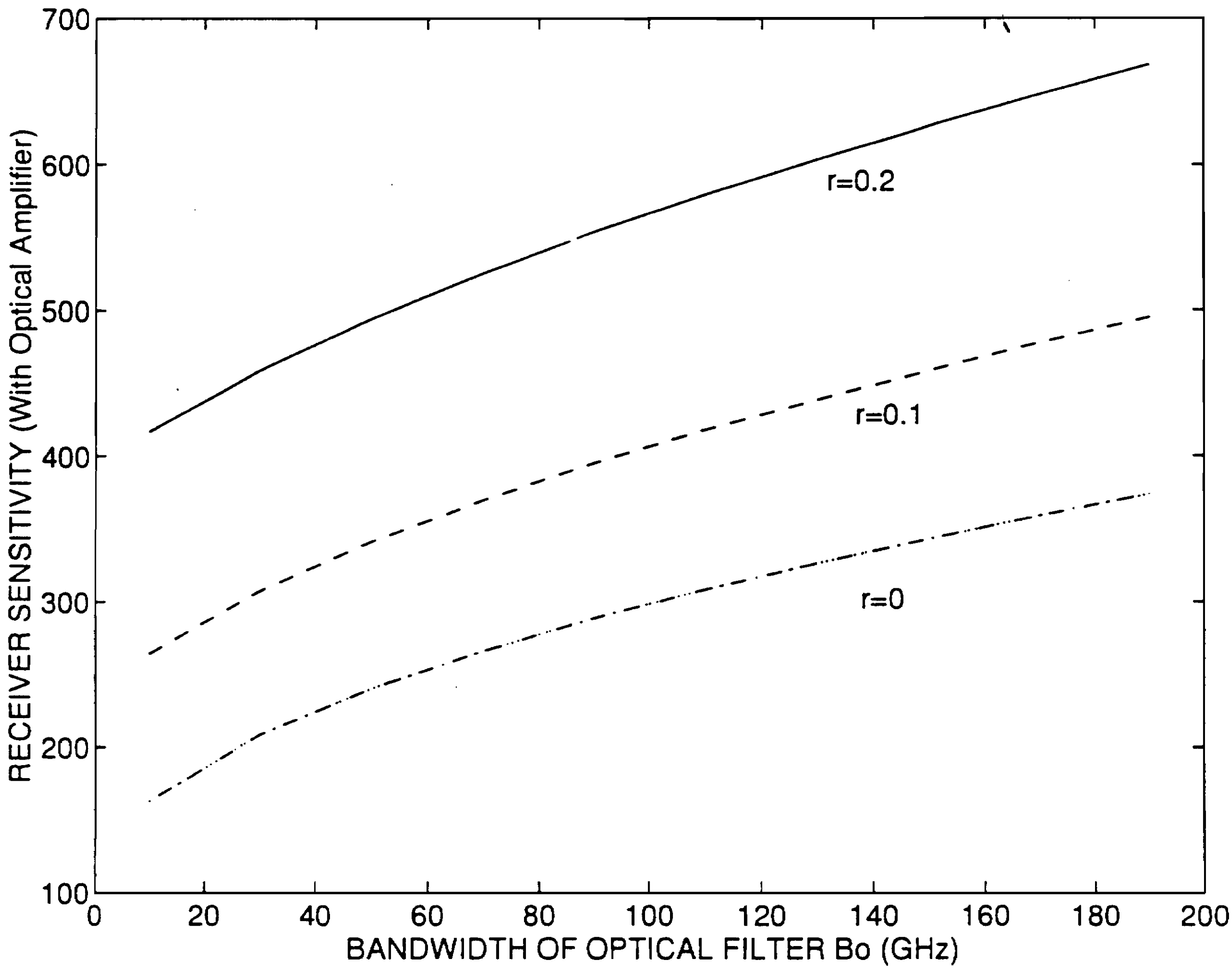

FIGURE A.4 RECEIVER SENSITIVITY vs. OPTICAL BANDWIDTH

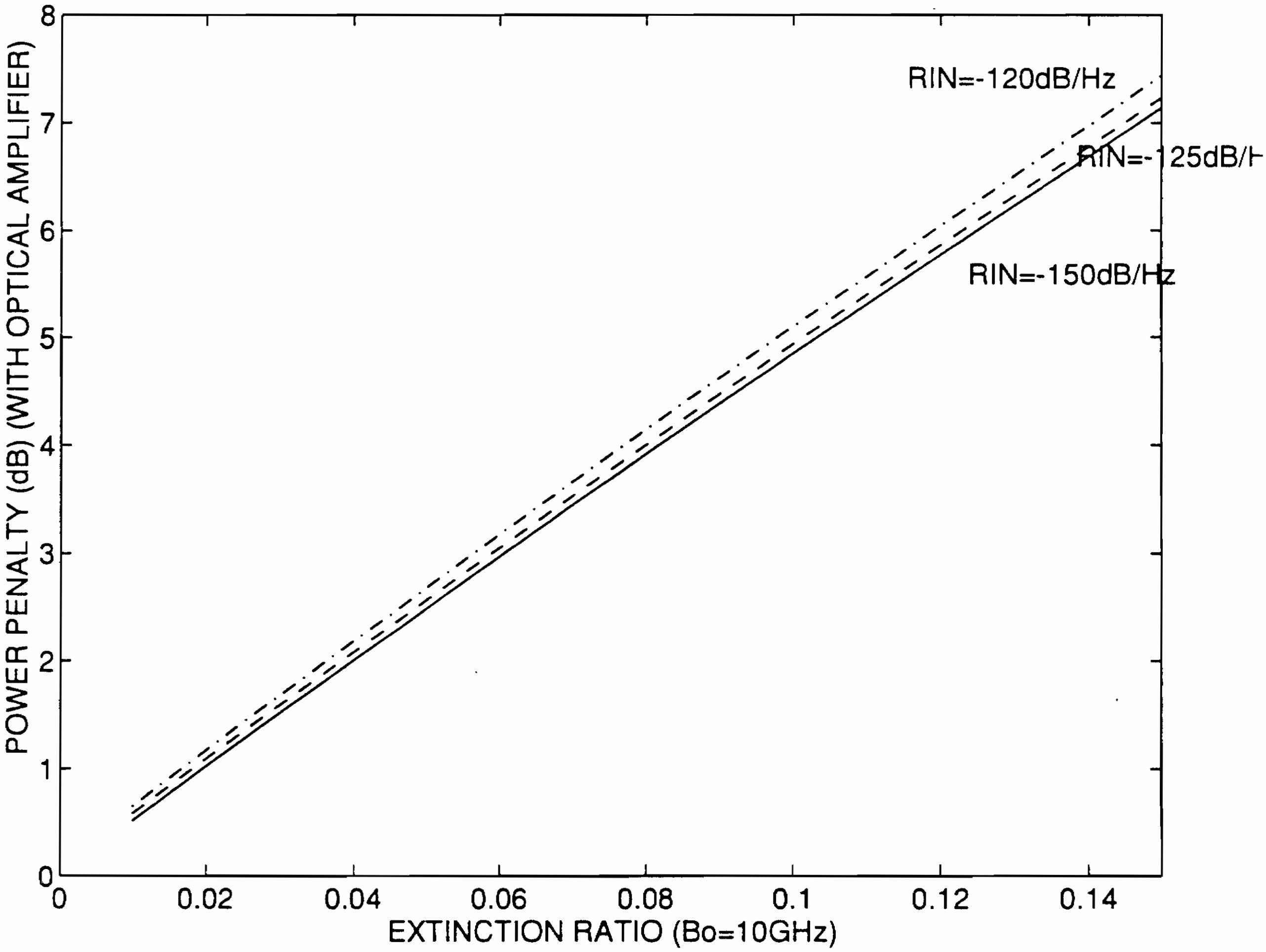

FIGURE A.5 COMBINED EFFECT OF RIN & NON-ZERO EXTINCTION RATIO

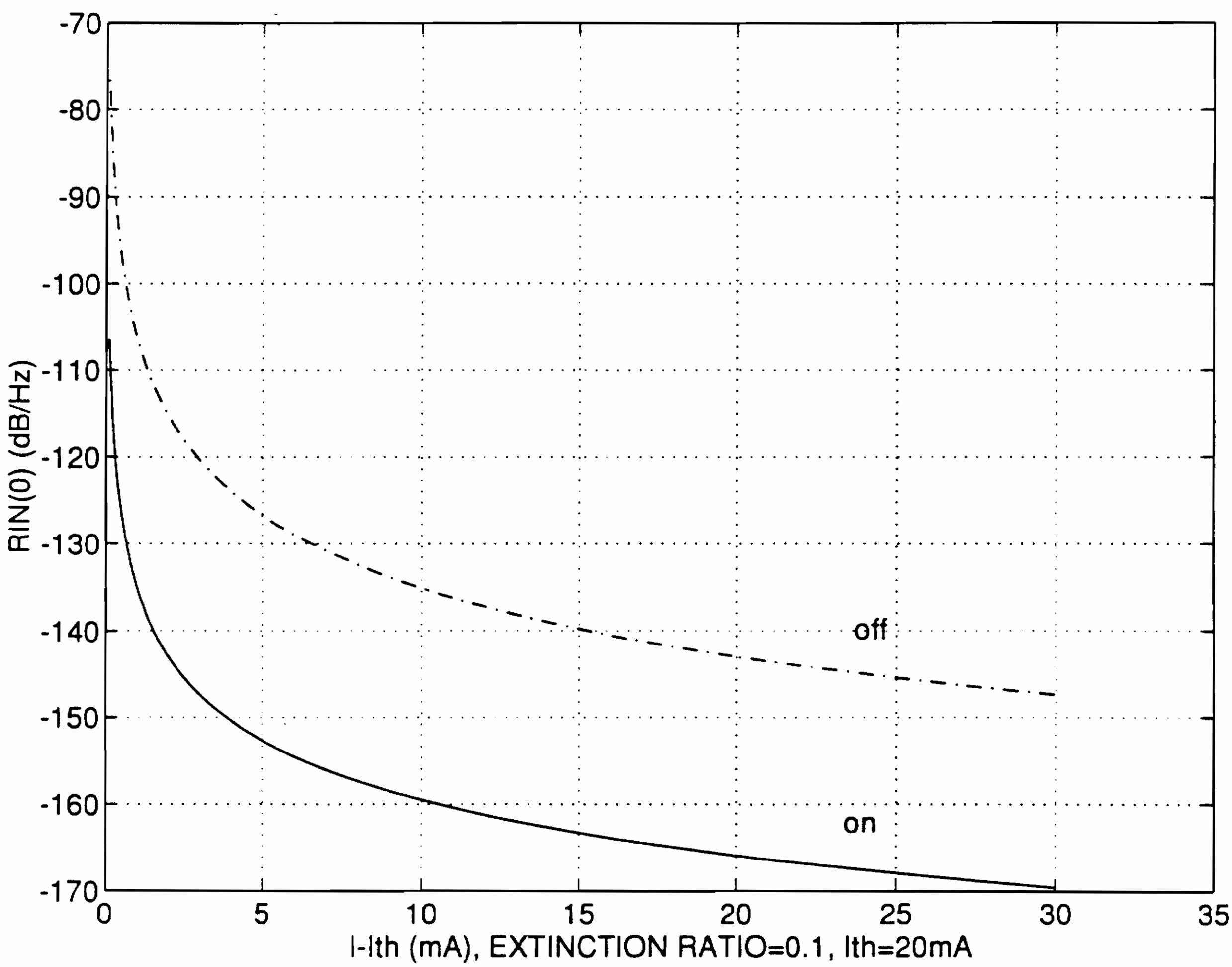

FIGURE A.6 RIN(0) IN ON AND OFF STATES WITH NON-ZERO EXTINCTION RATIO

References:

[1] T. E. Darcie, M. E. Dixon, B. L. Kasper, and C. A. Burrus, "Lightwave systems using microwave subcarrier multiplexing," Electron. Lett., Vol. 22, pp. 74-775, 1986.

[2] R. Olshansky, V. A. Lanzisera, "60-channel FM video subcarrier multiplexd optical communication system," Electron. Lett., Vol. 23, pp. 1196, 1987.

[3] W. I. Way, R. S. Wolff, and M. Krain, "A 1.3mm 35km fiber-optic microwave multicarrier transmission system for satellite earth stations," J. Lightwave Tech., Vol. LT-5, No. 9, pp. 1325-1332, 1987.

[4] T. Darcie and G. Bodeep, "Lightwave subcarrier CATV transmission systems," IEEE Trans. Microwave Theory Tech., Vol. 38, pp. 524, 1990.

[5] A. A. M. Saleh, "Fundamental limit on number of channels in SCM lightwave CATV system," Electron. Lett., vol. 25, no. 7, pp. 776-777, 1989.

[6] M. Tanabe, T. Uno, K. Kaida, H. Nakata, K. Fujito, and T. Ichida. "80 ch. AM-FDM signals optical transmission," LEOS Summer Topical Conf. Dig., BAM6, pp. 18-19, Monterey, Calf., July 1990.

[7] C. Chung & I. Jacobs, "Practical TV channel capacity of lightwave multichannel AM SCM systems limited by the threshold nonlinearity of laser diodes", IEEE Photonic Tech. Lett., Vol. 4, No. 3, pp. 289-292, March 1992.

[8] W. I. Way, M. M. Choy, A. Yi-Yan, M. Andrejco, M. Saifi, and C. Lin, "Multichannel AM-VSB television signal transmission using an erbium-doped optical fiber power amplifier," IEEE Photon. Tech. Lett., Vol. 1, pp. 343, 1989.

[9] P. M. Gabla, V. Lamaire, H. Krimmel, J. Otterbach, J. Auge, and A. Dursin, "35 AM-VSB TV channels distribution with high signal quality using a 1480nm diode-pumped erbium-doped fiber postamplifier," IEEE Photon. Tech. Lett., Vol. 3, pp. 56, 1991.

[10] A. Willner, et. al., "Star couplers with gain using multiple erbium-doped fibers pumped with a single laser", IEEE Photonic Tech. Lett., Vol. 3, No. 3, pp. 250-252, March 1991.

[11] A. A. M. Saleh, etc., "Modeling of Gain in Erbium-Doped Fiber Amplifiers,", IEEE Photon. Tech. Lett., Vol. 2, No.10, October 1990.

[12] I. Jacobs, "Optical amplifier noise figure", Memorandum to Bellcore, June 1993.

[13] N. Olsson, "Lightwave systems with optical amplifiers", J. of Lightwave Tech., Vol. 7, No. 7, pp. 1071-1081, July 1989.

[14] C. J. Chung, "Practical performance and system capacity of lightwave AM SCM video systems," Ph. D Dissertation, Virginia Polytechnic Institute and State University, April, 1992.

[15] C. J. Chung and I. Jacobs, "Simulation of the effects of laser clipping on the performance of AM SCM lightwave systems," IEEE Photon. Technol. Lett., Vol. 3, pp. 1034-1036, Nov. 1991.

[16] K. Alameh and R. A. Minasian, "Ultimate limits of subcarrier multiplexed lightwave transmission," Electron. Lett., Vol. 27, No. 14, pp. 1260-1262, 1991.

[17] M. Lax, "Quantum Noise VII: The Rate Equations and Amplitude Noise in Lasers," IEEE J. Quantum Electro., QE-3, No. 2, pp. 37-46, February, 1967.

[18] G. P. Agrawal, *Fiber-Optic Communication Systems*, John Wiley & Sons, Inc., 1992.

[19] G. P. Agrawal & Dutta, *Long-wavelength Semiconductor Lasers*, Van Nostrand Reinhold Company, 1986.

[20] Mukai, T., and Y. Yamamoto, "AM Quantum Noise in 1.3μm InGaAsP lasers," Electronics Letters, Vol. 20., pp. 29, 1984.

[21] J. L. Gimlett and N. K. Cheung, "Effects of phase-to-intensity noise conversion by multiple reflections pm gigabit-per-second DFB laser transmission systems," J. Lightwave Technol., Vol. 7, No.6, June 1989.

[22] C. H. Henry, "Theory of the linewidth of semiconductor lasers," IEEE J. Quantum Electron., Vol.. QE-18, No. 2, pp. 259-264, February 1992.

[23] M. Kobayashi, T. Ishihara, and M. Gotoh, "Power penalty due to optical reflections in erbium-doped fiber preamplifer," IEEE Photonics Technol. Lett., Vol. 5, No.8, August 1993.

[24] P. W. France (edited), *Optical Fiber Lasers and Amplifiers*, CRC Press, Inc., Boca Raton, Florida, 1991.

[25] A. Kelkar, "Dynamic range limitations of analog fiber optic links for mobile applications," Master Thesis, July, 1994.

[26] K. Kikushima, and H. Yoshinaga, "Distortion due to gain tilt of erbium-doped fiber amplifiers," IEEE Photonic. Technol. Lett., Vol. 3, No. 10, pp. 945-947, Oct. 1991.

[27] K. Kikushima, "AC and DC Gain Tilt of Erbium-Doped Fiber Amplifiers," J. Lightwave Technol., Vol. 12, No. 3, March 1994.

[28] G. P. Agrawal, *Nonlinear Fiber Optics*, Academic Press, San Diego, CA 1989

[29] R. W. Tkach, "Strategies for coping with fiber nonlinearities in lightwave systems," Tutorial Sessions of OFC'94, San Jose, CA 1994.

[30] C. Giles & E. Desurvire, "Modeling Erbium-doped fiber amplifiers", J. of Lightwave Tech., vol. 9, No. 2, pp. 271-283, February 1991.

[31] I. Habbab, etc., "Optimized performance of erbium-doped fiber amplifiers in subcarrier multiplexed lightwave AM-VSB CATV systems", J. of Lightwave Tech., Vol. 9, No. 10, pp. 1321-1329, October 1991.

VITAE

David Yong Chen was born on November 17, 1968 in Nanping, Fujian, China. In 1986, he finished eleven year primary and secondary education at the school where his father was the principal. Then he entered Xiamen University to study Semiconductor Physics. As a junior, he was elected as the chairman of the Student Union of Physics Department. In July, 1991, a year after obtaining his Bachelor's degree, he began his study in the United States. After one year graduate study in the Physics doctoral program at University of South Carolina, he transferred to the department of Electrical Engineering at Virginia Polytechnic Institute and State University in August, 1992. At Virginia Tech, he completed his study for a Master's degree in August, 1994. He is receiving further education and trying to pursue his engineering career in the field of telecommunications. He loves singing songs and playing soccer.

David Yong Chen